

Stability and adhesion properties of *Lacticaseibacillus rhamnosus* GG embedded in milk protein cryogels: Influence of plant seed gum inclusion

Thierry Hellebois^{a,b}, Jennyfer Fortuin^{a,c}, Sébastien Cambier^a, Servane Contal^a, Céline C. Leclercq^a, Claire Gaiani^b, Christos Soukoulis^{a,*}

^a Environmental Research and Innovation (ERIN) Department, Luxembourg Institute of Science and Technology (LIST), 5 Avenue des Hauts-Fourneaux, Esch-sur-Alzette, L4362, Luxembourg

^b Université de Lorraine, LIBio, F54000, Nancy, France

^c Food Quality and Design Group, Wageningen University and Research, NL6708, Wageningen, the Netherlands

ARTICLE INFO

Keywords:

Cryogel
L. rhamnosus GG
 Storage
 In vitro digestion
 Adhesion
 Bioactive peptides

ABSTRACT

This work reports on the influence of plant seed gum (PSG) from alfalfa (*Medicago sativa* L.) and flaxseed (*Linum usitatissimum* L.) on cryogels based on sodium caseinate (NaCas), whey protein isolate (WPI), and their combined mixture in embedding the probiotic *Lacticaseibacillus rhamnosus* GG (LGG). A significant preservation of LGG cell viability was achieved during the xero-structuration process. Among the materials tested, sodium caseinate was the standout, most effectively preserving LGG's biological activity across varying temperature and humidity conditions. Elevated storage temperature and relative humidity conditions accelerated LGG inactivation rates, especially in the case of WPI (in the presence or absence of PSG), which was primarily attributed to increased metabolic activity due to the changes in the xero-scaffolds' physical state. Moreover, the specific protein type used played a pivotal role in determining LGG's survival rates during simulated gastrointestinal digestion processes. In adhesion tests using a Caco-2/HT-29 co-culture model, LGG showed the highest adhesion found in NaCas. Interestingly, except for NaCas, adding PSG augmented LGG's bioadhesion capabilities, with flaxseed gum showing the highest enhancement in adhesin-mucin interactions. The research also underscored the release of bioactive peptides, which displayed a range of health benefits including antimicrobial and antioxidant properties.

1. Introduction

Galactomannans and mucilages are the most prevalent gums found in the endosperm and outermost seed coat layer of plant seeds, respectively (Cakmak et al., 2023; Kontogiorgos, 2019; Lira et al., 2023; Prajapati et al., 2013; Qian, Cui, Wu, & Goff, 2012; Soukoulis, Gaiani, & Hoffmann, 2018; Wu, Cui, Eskin, & Goff, 2009). It was previously demonstrated that the endosperm of alfalfa seeds (*Medicago sativa* L.) is rich in a galactomannan (mannose-to-galactose ratio ~ 1.18), which exhibits satisfactory thickening, gelling and cryogel-forming properties (Hellebois, Gaiani, Cambier, Noo, & Soukoulis, 2022; Hellebois, Soukoulis, et al., 2021). On the other hand, flaxseed (*Linum usitatissimum* L.) is one of the most studied plant seed mucilages composed of a high molecular weight (>1500–2000 kDa) arabinoxylan (AX) fraction, a low molecular weight (<500 kDa) rhamnogalacturonan-I based fraction and two intermediate molecular weight (500–2000 kDa) AX-RG-I

composite fractions (Hellebois, Fortuin, et al., 2021). Heretofore, flaxseed gum has been successfully employed as food thickener, gelling and stabilising agent (Liu, Shim, Tse, Wang, & Reaney, 2018), whereas its immunoregulatory, *anti*-glycaemic, *anti*-lipidemic and anti-obesity functions have been well documented (Luo et al., 2018; Mueed et al., 2022).

Numerous studies have highlighted that imbalances in the gut microbiome are tied to a range of health issues, including chronic inflammation, obesity, type-II diabetes, various cancers, and irritable bowel syndrome (IBS) (Torres-Fuentes, Schellekens, Dinan, & Cryan, 2017; Venema & Carmo, 2015). A common treatment is the use of probiotics, sometimes combined with soluble dietary fibres. The International Scientific Association for Probiotics and Prebiotics (ISAPP) defines "probiotics" as specific microbial species that, when administered in adequate amounts confer a health benefit on the host (Hill et al., 2014).

* Corresponding author.

E-mail address: christos.soukoulis@list.lu (C. Soukoulis).

<https://doi.org/10.1016/j.foodhyd.2024.109867>

Received 31 October 2023; Received in revised form 26 January 2024; Accepted 5 February 2024

Available online 9 February 2024

0268-005X/© 2024 The Authors. Published by Elsevier Ltd. This is an open access article under the CC BY license (<http://creativecommons.org/licenses/by/4.0/>).

Encapsulation, i.e., the physicochemical entrapment of bioactive compounds and/or living cells (such as probiotics) in bespoke soft matter templates, is widely employed for the oral delivery of probiotics. Dry particulates, hydrogels, bigels, and cryogels have been designed to protect the cells against physical and chemical stressors (Cook, Tzortzis, Charalampopoulos, & Khutoryanskiy, 2012; Garcia-Brand et al., 2022; Gu et al., 2022; Haji, Cheon, Baek, Wang, & Tam, 2022). A range of biopolymers, including proteins, starch and its derivatives and various gums as well, have been deployed for crafting the wall material of probiotic formulations (Burgain, Gaiani, Cailliez-Grimal, Jeandel, & Scher, 2013; sekhavatzadeh, Pourakbar, Ganje, Shekarfroush, & Hosseinzadeh, 2023; Zhu et al., 2023). The use of binary protein – polysaccharide wall materials is known to enhance the mechanical and barrier (i.e. oxygen and water vapour permeation) properties of the carrier matrix, thereby enhancing the survivability of the probiotic cells during storage, allowing their targeted release and mediating their adhesion to the gut mucosa layer (de Melo Pereira, de Oliveira Coelho, Magalhães Júnior, Thomaz-Soccol, & Soccol, 2018; Sanders & Marco, 2010).

Cryogels are macroporous carriers of customisable microstructure, mechanical strength, and high biocompatibility and biodegradability crafted through the freeze-drying a polymeric precursor specifically physically or chemically cross-linked to form hydrogels (Lozinsky, 2018; Manzocco, Mikkonen, & García-González, 2021). Cryogels offer multifaceted applications in the food industry such as the encapsulation and targeted delivery of bioactive compounds and living probiotic cells (Fontes-Candia et al., 2022; Hellebois, Canuel, Leclercq, Gaiani, & Soukoulis, 2024; Kleemann, Selmer, Smirnova, & Kulozik, 2018, 2020; Manzocco et al., 2021; Volkova & Berillo, 2021). It was recently demonstrated that milk protein based cryogels are excellent carriers to promote the biological activity of *Lactocaseibacillus rhamnosus* GG cells during the cryostructuring process and against diverse physicochemical stressors associated with storage and in vitro digestion (Hellebois, Canuel, et al., 2024). The incorporation of soluble dietary fibres such as pullulan (Sun et al., 2021) and sodium alginate (Kuo, Clark, Qin, & Shi, 2022) in freeze-dried hydrogels was associated with enhanced survivability of the embedded probiotic cells (*L. plantarum* or *L. acidophilus* and *B. lactis*, respectively) during processing, storage and in vitro digestion.

In the present work, we aimed to provide insights into the functional role of plant seed derived gums as co-structuring wall material in milk protein cryogel templates for the oral delivery of probiotic cells. In view of this, alfalfa and flaxseed gums were assessed for their ability to preserve the survivability of *Lactocaseibacillus rhamnosus* GG living cells, under controlled storage and in vitro digestion simulated conditions and mediating their bioadhesion into a Caco-2/HT-29 mucin producing co-culture cell model of the intestinal epithelium. In addition, the potential of the probiotic cryogels in providing supplementary health benefits associated with the release of bioactive peptides was assessed by means of omics tools.

2. Materials and methods

2.1. Materials

Whey protein isolate (WPI) powder (PRODIET 90 S) with a protein content of 85.8% wt. (wet basis) was kindly donated by Ingredia (Arras, France). Sodium caseinate (NaCas) containing 89.4% wt. Of protein (N % × 6.25, wet basis), glucose (99.5% wt.) and glycerol (99.9% wt.) was purchased from Sigma-Aldrich (Leuven, Belgium). Trehalose (99.4% wt.) was obtained from Louis-François (Croissy-Beaubourg, France). The De Man, Rogosa and Sharpe (MRS) culture media was purchased from Carl Roth (Karlsruhe, Germany). The probiotic strain *Lactocaseibacillus rhamnosus* GG (LGG) ATCC 53103 used was purchased from VTT Technical Research Centre of Finland Ltd (Espoo, Finland). All the other chemicals used were of analytical grade.

2.2. Preparation of the *Lactocaseibacillus rhamnosus* GG embedding cryogel monoliths

The procedure for preparing the milk protein-based cryogels is detailed in Hellebois et al. (2023). Briefly, a solution was formulated with 10% wt. in protein content consisting of sodium caseinate (NaCas), whey protein isolate (WPI), or a binary (1:1) mixture of NaCas and WPI, in addition to 5% wt. trehalose, 2.5% wt. glycerol, and 1% wt. glucose. After undergoing heat treatment at 80 °C for 20 min, either alfalfa seed gum (AAG) or flaxseed gum (FG) was incorporated into the hot protein solution at concentrations of 0.1% or 0.5% wt., before being left to solubilise overnight. Subsequently, the protein solutions were gelled via indirect acidification by LGG (end of the exponential phase) fermentation at approximately 9.3 logCFU.mL⁻¹ for a period of 4 h at 37 °C. Finally, the solutions were frozen at –80 °C for 2 h and then freeze-dried for 40 h (Hellebois et al., 2023).

2.3. Viable *Lactocaseibacillus rhamnosus* GG quantification

The total viable counts (TVC) of LGG were determined utilising the method delineated in Hellebois, Addiego, Gaiani, Shaplov, and Soukoulis (2024). Concisely, aliquots, each constituting either 1 mL of the inoculated protein solution at t = 0 min, 1 mL of the fermented hydrogel at t = 240 min, 1 g of freeze-dried cryogels, or 1 mL of digestive chymes, were serially diluted by a factor of ten in phosphate-buffered saline (PBS). These diluted solutions were subsequently cultured on MRS agar plates. To simulate microaerophilic conditions, the plated sample was overlaid with a fine layer of MRS agar, followed by incubation at 37 °C for 48 h.

2.4. *Lactocaseibacillus rhamnosus* GG storage stability

To assess the storage stability of LGG cells, freshly produced cryogel monoliths were transferred into hermetically sealed Nalgene acrylic desiccator cabinets (Thermo Fisher Scientific, Waltham, MA, United States). The effect of the physical state of the cryogels (glassy vs. rubbery) was tested using saturated salt solution – LiCl (a_w = 0.11) and NaCl (a_w = 0.75) – at a constant temperature of 20 °C. The effect of the temperature was assessed in the glassy state using LiCl saturated salt solution at 5, 20 and 37 °C. The resulting LGG inactivation data was then fitted to the Weibull's model (van Boekel, 2002) as follows:

$$\log S_t = -\frac{1}{2.303} \left(\frac{t}{\alpha} \right)^\beta \quad (1)$$

where t is the corresponding time (d), S(t) the LGG survival ratio (N_t/N_{initial}) at t days, α a constant describing the time (in days) required to observe a reduction of 0.434 logCFU.g⁻¹ of the initial counts (N_{initial}) and β a constant describing the model's curvature. From Eq. (1), can be obtained the following equation:

$$t_{\text{shelf-life}} = \alpha \left(-\ln(10^{-(N_{\text{initial}}-6)}) \right)^{\frac{1}{\beta}} \quad (2)$$

Where α and β are analogous with Eq. (1), t_{shelf-life} is the shelf-life (i.e. reduction to 6 logCFU.g⁻¹) time (in days) and N_{initial} the LGG counts at t = 0 day. Due to the limited bacterial loss during the storage, a first-order kinetic model (Eq. (3)) was applied in the case of cryogels stored at 5 °C a_w 0.11 as follows:

$$\log N_t = \log N_{\text{initial}} - kt \quad (3)$$

Where N₀ and N_t are the number of living LGG cells at t = 0 day and t = t day, respectively and k the inactivation rate constant (day⁻¹). From Eq. (3) the shelf-life (in days) was calculated as follows:

$$t_{\text{shelf-life}} = \frac{(\log N_{\text{initial}}) - 6}{|k|} \quad (4)$$

Where $t_{\text{shelf-life}}$ and N_{initial} are analogous to Eq. (2) and k is analogous to Eq. (3).

2.5. In vitro digestion

2.5.1. In vitro digestion protocol

The INFOGEST v2.0 in vitro simulated digestion protocol (Brodtkorb et al., 2019) was implemented to access the protein hydrolysis and microstructure as well as the bacteria viability. Minor modifications to the protocol were applied and are specifically described in our previous study (Hellebois, Canuel, et al., 2024).

2.5.2. Microscopical assessment of the digesta

To monitor the colloidal changes of the proteins as well as qualitatively visualise the bacterial lethality during the in vitro digestion, aliquots (1 mL) of gastric ($t = 120$ min) and intestinal ($t = 120$ min) chyme suspension were non-covalently stained and the following fluorophores were used: 10 μL of 0.05% Fast Green for proteins, 1.5 μL of 3 mM Syto9 for living cells, and 1.5 μL of 20 mM propidium iodide for inactivated cells. Three hundred microliters were then transferred onto eight-well Nunc Lab-Tek II microscope slides and were microscopically assessed using a $\times 40$ objective lens mounted on a confocal laser scanning microscope (LSM 880 with Airy scan, Zeiss, Jena, Germany).

2.5.3. Proteomic and peptidomic analyses

The cleavage of the proteins in the intestinal ($t = 120$ min) chymes was monitored by capillary sodium dodecyl sulfate–polyacrylamide gel electrophoresis (SDS-PAGE). The electrophoresis was run using a Bio-analyzer 2100 with the protein 80 chip kit following the manufacturer instructions (Agilent Technologies, Santa Clara, CA, United States). The gels were reconstructed using 2100 Expert software (Agilent Technologies, Santa Clara, CA, United States).

To determine the production of peptides from the milk proteins at the end of the in vitro digestion, 10 mL aliquots of homogeneous intestinal chymes were centrifuge-filtered. Amicon tubes (Merck, Darmstadt, Germany) equipped with a filter cut-off of 10 kDa were used to remove the uncleaved proteins. Then, 1 mL of the filtrates obtained were vacuum-dried (CentriVap, Labconco, Kansas City, MO, United States) and analysed using nano-liquid chromatography – mass spectrometry (nano-LC-MS) analyses following the method described in Hellebois, Addiego, et al. (2024). The significant peptide sequences (score ≥ 50) obtained were then compared to the bioactive peptide database BIOPEP-UWM (Minkiewicz, Iwaniak, & Darewicz, 2019).

2.5.4. Mucoadhesion behaviour of *Lacticaseibacillus rhamnosus* GG cells

2.5.4.1. Preparation of the intestinal epithelium coculture model. The human colon cancer Caco-2 cell line sub-clone TC7 (Caco-2/TC7) and HT29-MTX cells lines were maintained in Dulbecco's Modified Eagle Medium-Glutamax (DMEM-Glutamax, Invitrogen, Merelbeke, Belgium) supplemented with 10% fetal bovine serum (Invitrogen, Merelbeke, Belgium) at 37 ± 0.5 °C in 10% CO_2 atmosphere in a humidified incubator. Their co-culture was initiated by seeding the cells at a 90:10 ratio (Caco-2/TC7 and HT29-MTX respectively) and were grown for 14 days at 37 ± 0.5 °C in a 10% CO_2 humidified incubator (Georgantzopoulou et al., 2016). The medium was replaced every two days. At the end of the 14 days of differentiation the medium was discarded, and the differentiated co-culture cell line was washed with PBS. To prevent the digestion of the Caco2/HT29 epithelium model in the presence of the intestinal enzymes (trypsin), the cells were fixated using 2.5% vol. glutaraldehyde in PBS for 30 min at 25 ± 1 °C. The glutaraldehyde was washed-out by sequential PBS washings.

2.5.4.2. Assessment of adhered *Lacticaseibacillus rhamnosus* GG cells. To investigate the adhesion potential of the LGG cells on the intestinal

epithelium, PBS was replaced by intestinal chymes ($t = 120$ min) of the cryogels i.e. 300 μL in eight-chambered microscope slides (Nunc Lab-Tek II, Thermo Fisher Scientific, Waltham, MA, United States) or 2500 μL in six-well microplates (Corning, Corning, NY, United States) for the microscopic assessment and TVC, respectively. After 120 min of incubation at 37 ± 1 °C in an orbital shaker (100 rpm) (Świątecka, Małgorzata, Aleksander, Henryk, & Elżbieta, 2010), the systems were washed twice with PBS. The microscopic evaluation of the adhesion of the bacteria onto the mucosa was assessed in wet conditions using a $\times 40$ objective mounted on a CLSM microscope (LSM 880 with Airy scan, Zeiss, Jena, Germany). Fast Green, SYTO9, and propidium iodide were added as staining agents for protein, viable and inactivated LGG cells, respectively. Simultaneously, a twin system was immobilised using a 2.5% volume of glutaraldehyde in PBS for a duration of 30 min at a temperature of 25 ± 1 °C. The solvent was replaced through a sequential washing process, transitioning from water to ethanol, with concentrations of 10, 30, 50, 70, and 90% employed once, and 100% ethanol three-fold. To preserve the tissue integrity, an ethanol–hexamethyldisilazane (HMDS) solvent exchange was performed. The system was washed once with 10, 30, 50, and 70% HMDS, followed by three washes with 90 and 100% HMDS. The solvent was evaporated overnight at room temperature, and the systems were then affixed to a carbon tape, coated with a 5 nm layer of platinum using an ACE 600 coating system from Leica Microsystems (Wetzlar, Germany) and stored in a desiccator to prevent water absorption until further use. Scanning electron microscopy (SEM) was conducted using a field emission scanning electron microscope (SU-70, Hitachi, Tokyo, Japan). The acceleration was set to 5 kV, with a working distance of 15 mm and a magnification of $\times 5000$.

To enumerate the cultivable adhered LGG cells, the epithelium model was mechanically disrupted in PBS, allowing the bacteria to be released. Subsequently, the bacteria suspensions were plated onto MRS agar medium, which was then overlaid with a second layer of MRS agar. The plated samples were incubated at a temperature of 37 °C for a duration of 2 days.

2.6. Statistical analyses

The normal distribution of the data was assessed using the Shapiro-Wilk test and Q–Q plot visual representations. To identify significant variances, a one-way ANOVA was conducted employing the Origin 2019b software (OriginLab Inc., Northampton, MA, United States). Upon detecting significant differences ($p < 0.05$), Tukey's post-hoc test was employed to differentiate between mean values.

3. Results and discussion

3.1. Viability of the *Lacticaseibacillus rhamnosus* GG during freeze-drying

The impact of the biopolymer composition on the viability of LGG throughout the cryostructuring process (i.e. hydrogel formation and freeze-drying) is illustrated in Fig. 1. According to the ANOVA findings, only the protein type was significantly influential on the total viable counts of LGG, with the survivability rates being proportionally increasing to the increase in the NaCas to WPI mass fraction ($m_{\text{NaCas}}/w_{\text{WPI}}$). As expected, the fermentation of the precursor solutions was associated with a significant – yet minor – increase in the TVCs of LGG, i.e. from 10.16 to 10.31 $\log\text{CFU}\cdot\text{g}^{-1}$. On the other hand, the freeze-drying of the hydrogel precursors was accompanied by a significant ($p < 0.001$) reduction in the TVCs of LGG ranging from 9.79 to 10.36 $\log\text{CFU}\cdot\text{g}^{-1}$ with the highest cellular sublethality being observed in the cryogels exerting the lowest $m_{\text{NaCas}}/w_{\text{WPI}}$. The survival rates of LGG during the freeze-drying step ranged from 41.7 to 83.2%, which is in keeping with the reported survival rates in protein – polysaccharides freeze-dried microtemplates (Oluwatosin, Tai, & Fagan-Endres, 2022).

As illustrated in the SEM micrographs (Fig. 2) in the absence of the

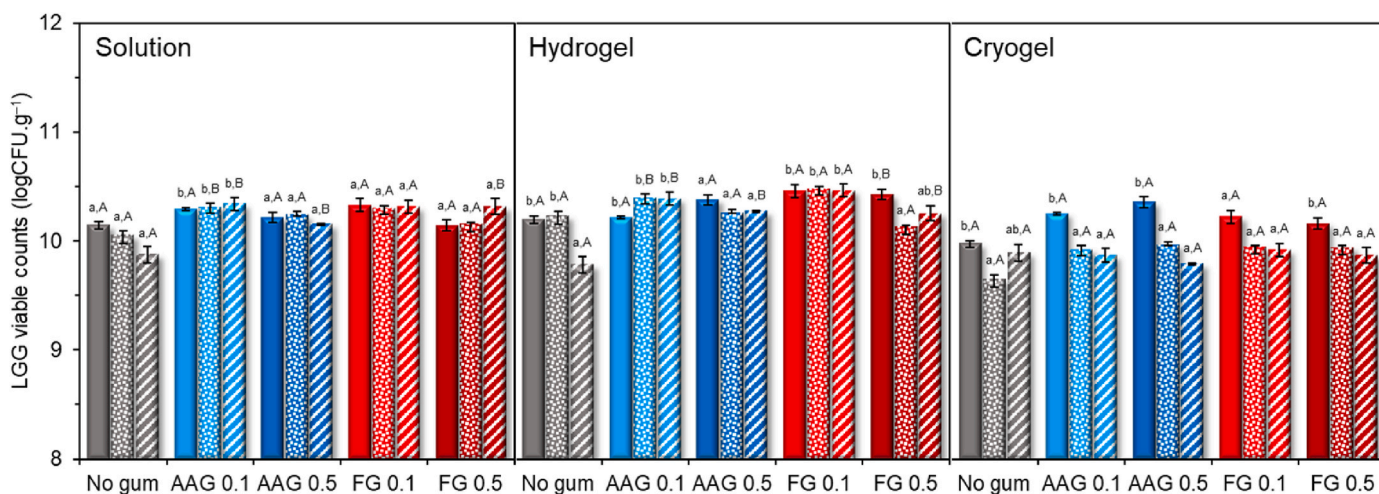


Fig. 1. *Lactiseibacillus rhamnosus* GG viable counts (logCFU.g⁻¹, expressed on dry basis) after inoculation of the protein solution (Solution), following 4 h of fermentation at 37 °C (Hydrogel) and after 40 h of freeze-drying (Cryogel). Plain bars: sodium caseinate (NaCas)-based cryogels, dashed bars: whey protein isolate (WPI)-based cryogels, dotted bars: Mixed protein cryogel with NaCas:WPI ratio of 1:1 (N1:1 W). AAG 0.1 and AAG 0.5: alfalfa gum at 0.1 and 0.5% wt., respectively. FG 0.1 and FG 0.5: flaxseed gum at 0.1 and 0.5% wt., respectively. ^{a-c}Different letters denote a significant (p < 0.05) difference between the protein type at the same state (lowercase) and for the different states for the same sample (uppercase) according to Tukey’s post hoc means comparison test.

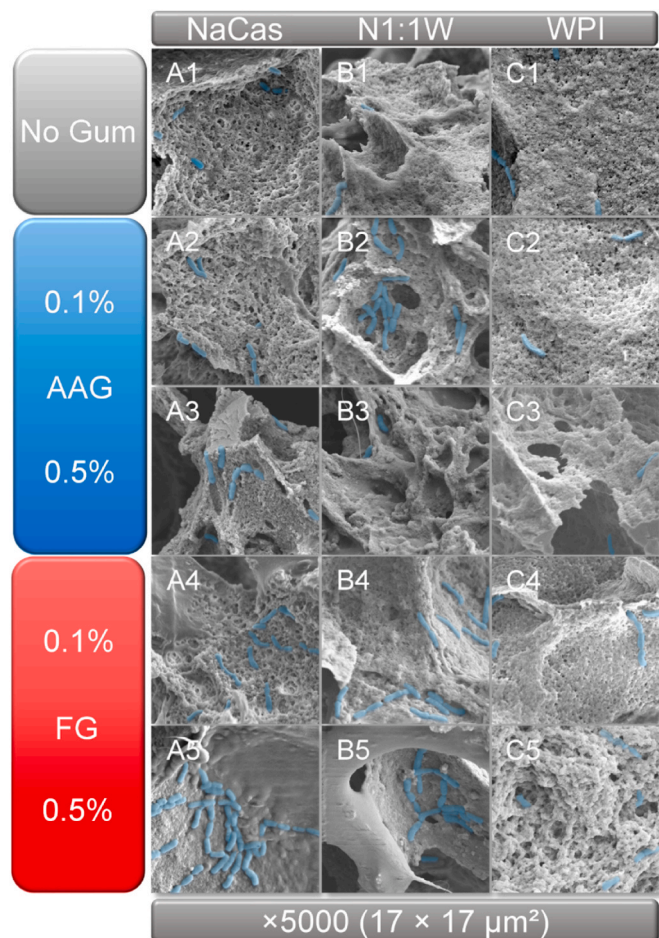


Fig. 2. Scanning electron microscopy images of sodium caseinate (A), mixed sodium caseinate – whey protein isolate at 1:1 ratio (B) and whey protein isolate (C)-based cryogels. Gum free systems are represented in “1”, cryogels containing alfalfa gum (AAG) at 0.1 and 0.5% in 2 and 3 and flaxseed gum (FG) at 0.1 and 0.5% in 4 and 5, respectively. For illustration purposes, the LGG cells were coloured in blue.

PSGs, the probiotic cells were well embedded into the protein-based skeleton of the cryogels with only few LGG chains residing on the outer surface. Interestingly, the inclusion of the PSGs in the cryogel precursors (hydrogels) resulted in an increase in the number of bacterial cells being deposited on the air – matrix interface (Fig. 2). The CLSM assisted visualisation of the microstructure of the probiotic solutions (Fig. 3) revealed that although the LGG cells show a preferential localisation in the protein-rich microdomains, the occurrence of segregative phase separation pushes some of the bacterial chains to the protein – PSG interface (most probably due to their differences in the osmotic pressure), which are ultimately immobilised during the indirect gelation process. These protein – PSG interface located bacteria appear to be the most sensitive to cellular damage taking place during the cryogenic processing (ice crystallisation of the PSG-rich aqueous pockets) and ice sublimation (dehydration is faster in the porogen microdomains). This may explain why the inclusion of the PSGs resulted in a higher (yet non-significant) reduction in the TVCs of LGG during the freeze-drying.

It is well demonstrated that the ability of the solutes to affect the colligative properties of the polymeric precursors as well as the ice crystal nucleation and ripening during the cryogenic processing step are inextricably associated with the achieved lyoprotective effects. In general, the frozen storage – glass transition temperature interval, i.e. $\Delta T = T_f - T_g$, is a significant determinant of the probiotics lethality due to the

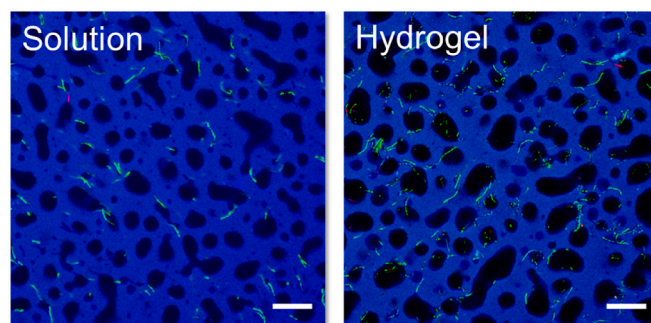


Fig. 3. Representative CLSM micrographs – WPI containing 0.1% of FG – of LGG cells localisation in milk protein-gum systems before and after lactic acid-induced gelation. Scale bar: 20 μm. Protein are stained in blue (fast green), living and dead bacteria in green and red, respectively. The gum microdomains are represented in black (unstained).

disruption of the cell membrane stemming from the uncontrolled growth of the ice crystals and the osmolytic stress (Guerrero Sanchez, Passot, Campoy, Olivares, & Fonseca, 2022; Kuo et al., 2022). As it was observed in our previous work (Hellebois, Addiego, et al., 2024), the measured T_g values for the gum-free systems was in the range of -34 to -36 °C, implying their complete vitrification under the implemented freezing conditions. In addition, the presence of the gums did not induce any remarkable change in the T_g values, due to their high effective molecular weight, which may also explain their non-significant impact on the attained lyoprotective effectiveness.

The presence of macromolecular lyoprotectants, i.e. compounds able to preserve the cells membrane fluidity during the dehydration process by binding water via hydrogen bonding in the vicinity of the polar interface of the phospholipid bilayer is another factor associated with the preservation of the biological activity of probiotics during lyophilisation (Aschenbrenner, Foerst, & Kulozik, 2015). In general, polysaccharides exert higher solvent (water) affinity compared to proteins due to the higher prevalence of polar side groups able to bind water via hydrogen bonding i.e., $-OH$ and $-COOH$. Although, some differences in the water affinity of the FG and AAG have been previously reported, i.e. $k_{Huggins} = 0.63$ and 0.85 , respectively (Hellebois, Fortuin, et al., 2021; Hellebois, Soukoulis, et al., 2021), it was not possible to identify any clear association with the survivability of LGG, which could be ascribed to their quite low mass fraction ($m_{PSG} = 0.5\text{--}2.6$ g.100 g⁻¹ dry solids). On the contrary, a good correlation between the surface hydrophobicity (i.e. 2.65 and 3.65 $\mu\text{g SDS.500 } \mu\text{g}^{-1}$ for NaCas and WPI, respectively) (Hiller & Lorenzen, 2008) and the solvent affinity (i.e. $k_{Huggins} = -1.33$ and -0.04 for NaCas and WPI, respectively) (O'Sullivan, Arellano, Pichot, & Norton, 2014) of the milk proteins and the survivability of LGG was found, suggesting that NaCas is more effective in binding water molecules than WPI. In keeping with this it was previously demonstrated that the NaCas based cryogels exhibited a higher water vapour sorption capacity compared to their WPI counterparts (Hellebois, Addiego, et al., 2024).

3.2. Storage stability of *Lactacisbacillus rhamnosus* GG

To assess the ability of the grafting xero-scaffolds to preserve the biological activity of the LGG cells under diversified static storage conditions, the probiotic cryogels were transferred into temperature (5, 20 and 37 °C) – relative humidity (11 and 75%) controlled cabinets and stored for 100 days. The LGG cell inactivation dynamics are illustrated in Fig. 4 and Table 1. As expected, both storage temperature and relative humidity were highly influential on the survivability of LGG. To gain insight into the LGG cell inactivation kinetics, the TVC – storage time data were analysed using Weibull (Eq. (1)) and first-order (Eq. (3)) regression models. As shown in Table 1, only in the case of the cryogels stored at chilling conditions the LGG inactivation were described by first order kinetics. A similar behaviour was also reported by Fortuin et al. (2023) in protein (pea, whey, or Spirulina) – maltodextrin lyophilisates embedding LGG cells. In the context of microbial inactivation, the Weibull distribution is used to model the probability that a microorganism will be inactivated by a certain treatment or environmental condition at a given time (van Boekel, 2002). The determined kinetic parameters, α and β denote the time required for observing a $\log(1/e)$ decline in the viable microbial load and the responsiveness of the cells to the imposed stressor (i.e. adaptation or cellular damage accumulation), respectively. At chilling conditions, the LGG cells response to the physicochemical stressors was negligible, with the NaCas cryogels allowing the best cell stabilising effect ($k = 1.43 \times 10^{-3}$, 4.67×10^{-3} , 4.99×10^{-3} day⁻¹, for NaCas, N1:1 W and WPI, respectively), which is in agreement with our previous study (Hellebois, Canuel, et al., 2024). The elevation of the storage temperature resulted in a significant ($p < 0.001$) shortening of the cell inactivation lag phase as indicated by the α_T parameter ($\alpha_T = 14.5$ vs. 0.68 days, at 20 and 37 °C, respectively) due to acceleration of the LGG metabolic activity. The α_T parameter was highly

dependent on the protein composition of the cryogels with the NaCas-based exemplars showing the best LGG cell stabilising effect ($\alpha_T = 1.33$, 0.41 and 0.20 vs. 35.7 , 4.53 and 3.59 days, for NaCas, N1:1 W and WPI cryogels stored at 37 and 20 °C, respectively). As for the β_T values, the impact of storage temperature was dependent on the composition of the cryogels. In general, the convexity ($\beta_T < 1$) of the LGG curves was significantly higher in the N1:1 W and WPI cryogels, compared to NaCas LGG inactivation curves, which represented a linear to concave behaviour ($\beta_T = 0.993$ vs. 1.548 at 37 and 20 °C, respectively). As well depicted in Fig. 4, the inclusion of PSGs in the cryogel formulation enhanced the storage stability of LGG embedded in the NaCas based systems but it impaired the LGG sublethality in the mixed protein and WPI exemplars. This illustrates the ability of NaCas to prolong the LGG cell damage accumulation before lethality is being established.

In a manner akin to storage temperature, the increase in the storage relative humidity resulted in a significant ($p < 0.001$) decrease in the calculated kinetic parameters ($\alpha_{RH} = 14.5$ vs. 1.4 day and $\beta_{RH} = 1.01$ vs. 0.87 , at 11 and 75% RH, respectively), with the $m_{NaCas/WPI}$ being the only influential compositional factor ($\alpha_{RH} = 18.6$, 2.8 and 2.4 , and $\beta_{RH} =$ for NaCas, N1:1 W and WPI, respectively, $p < 0.001$). On the other hand, the presence of PSG was rather of minor importance, with the PSG concentration influencing only the β_{RH} ($\beta_{RH} = 0.86$, 0.86 and 1.07 , respectively, for 0, 0.1 and 0.5% wt., respectively, $p < 0.05$). Based on the aforementioned, the NaCas-based cryogels containing 0.5% of PSG appeared to be the most adaptable xero-scaffolds to diverse RH conditions. In addition, despite their substantial differences in their molecular and chemical structure configuration, both tested PSGs provided similar shielding capacity against temperature and water vapour stressors throughout storage.

It is well documented that the sublethality of probiotic cells throughout storage is species- and strain-dependent (Wendel, 2022). In addition, extrinsic parameters such as composition, microstructure and physical state of the conveying soft-matter template are of paramount importance for maximising the bacterial cells stabilisation during storage (Gbassi & Vandamme, 2012; Iravani, Korbekandi, & Mirzohammadi, 2015; Sanders & Marco, 2010). Concerning the scaffold composition, previous studies have underlined the importance of proteins in preserving probiotics due to their ability to promote the cell – matrix adhesion (Gomand et al., 2019) allowing a satisfactory embedment of the living cells into the wall material and thus, suppressing the diffusivity of oxygen and water vapour; both being powerful physicochemical stressors leading to irreversible changes in the cell membrane integrity. Although previous studies have shown that WPI possess a good cell stabilising role (Burgain, Corgneau, Scher, & Gaiani, 2015; Yin, Chen, Yuan, Liu, & Zhong, 2024), the inferior storage stability of LGG embedded in the WPI cryogels can be primarily attributed to their lower lyostabilising performance compared to the NaCas exemplars. This is in keeping with the observations of Guerrero Sanchez et al. (2022) who documented that the changes in the integrity of the cell membrane lipid bilayer occurring during the freeze-drying process have a predominant role on the stability of probiotics during storage.

The storage conditions were selected in a fashion that allowed the achievement two distinct physical states, i.e. rubbery (at 75% RH) and glassy (at 11% RH). It is well established that the achievement of a glassy state is an essential factor for maximising the probiotic cells preservation throughout storage due to the suppression of their metabolic activity (Aschenbrenner et al., 2015). In our previous study, we have demonstrated that the inactivation rate of LGG embedded in milk protein cryogels commenced to progressively accelerate at $a_w > 0.33$ due to the transition from the glassy to the rubbery state (Hellebois, Canuel, et al., 2024). According the calculated α_{RH} and β_{RH} parameters, the physical state transition shortened the LGG inactivation lag phase due to alleviation of the steric inhibitors of the metabolic activity and biochemical reactions (e.g. lipid oxidation) taking place during storage. The superior LGG stabilising effects of NaCas compared to WPI, may be attributed to

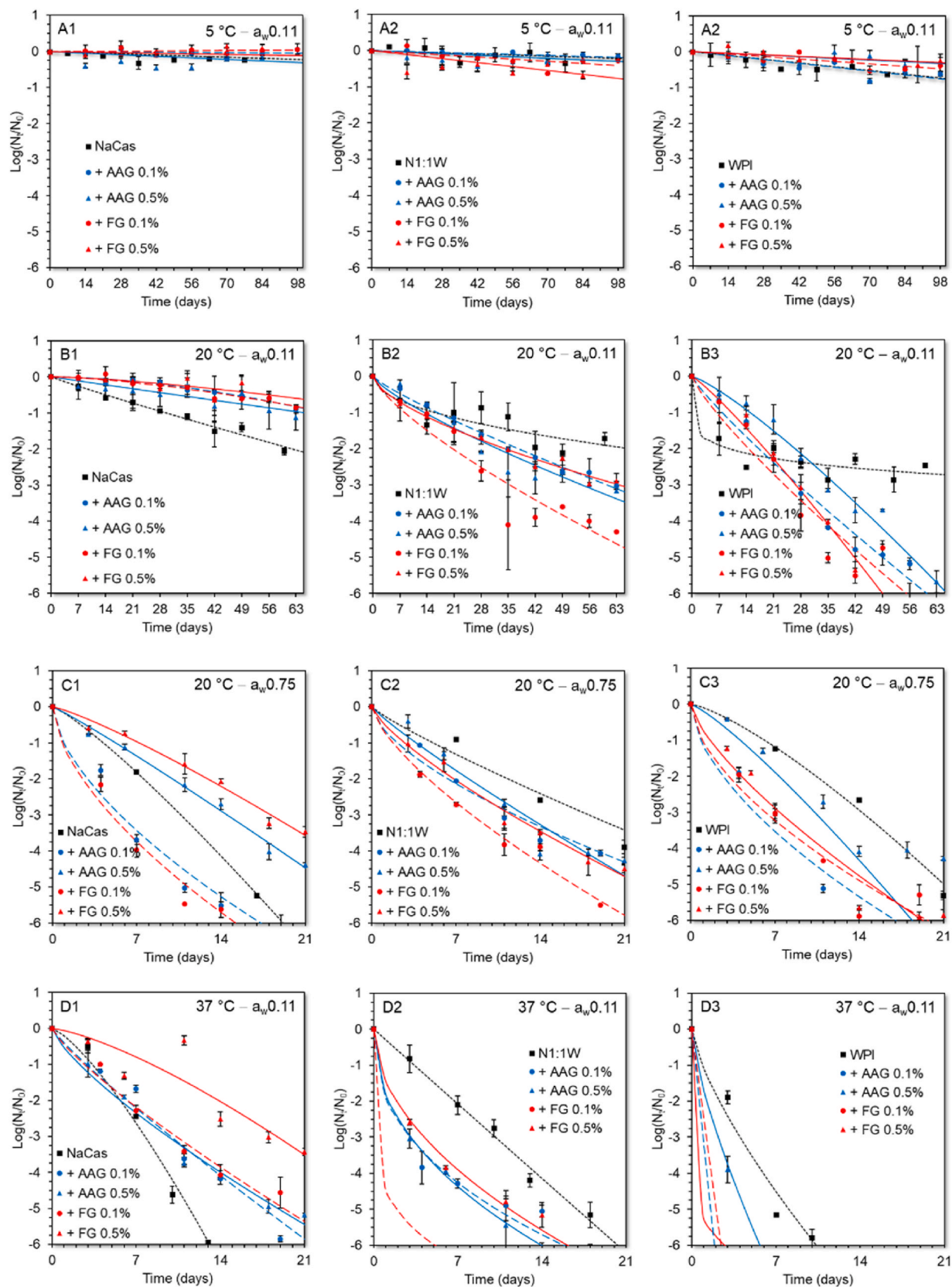


Fig. 4. LGG embedded in milk protein-based cryogels inactivation curves during storage at 5 °C, $a_w 0.11$ (A), 20 °C, $a_w 0.11$ (B), 20 °C, $a_w 0.75$ (C), 37 °C, $a_w 0.11$ (D). Sodium caseinate (NaCas)-based cryogels are found in “1”, mixed sodium caseinate – whey protein isolate at 1:1 ratio (N1:1W) in “2” and whey protein isolate (WPI) in “3”. First order (A) and Weibull’s model (B–D) fitted data are represented in black dotted lines for gum free cryogels, in dashed lines for 0.1% and continuous lines for 0.5%. Red: flaxseed gum, blue: alfalfa gum.

Table 1
LGG inactivation kinetic parameters influenced by the gum type and concentration, protein type and storage conditions.

Protein	Gum	¹ a _w 0.11		² a _w 0.11		² a _w 0.11		² a _w 0.75	
		5 °C		20 °C		37 °C		20 °C	
		Slope		α	β	α	β	α	β
		day ⁻¹		days	–	days	–	days	–
NaCas	No gum	–0.002 ^{bc}		12.07 ^{cd}		0.93 ^{abc}		1.77 ^{ab}	
	AAG 0.1	–0.001 ^{ab}		43.27 ^{ab}		1.72 ^a		1.11 ^{cd}	
	AAG 0.5	–0.003 ^{bc}		27.84 ^{bc}		0.98 ^{ab}		0.77 ^d	
	FG 0.1	–0.000 ^a		41.77 ^{ab}		1.52 ^{ab}		0.97 ^d	
	FG 0.5	–0.001 ^{abc}		50.72 ^a		1.42 ^{ab}		2.01 ^a	
N1:1 W	No gum	–0.002 ^c		2.85 ^d		0.49 ^{bc}		1.45 ^{bc}	
	AAG 0.1	–0.004 ^{bc}		6.26 ^d		0.85 ^{abc}		0.02 ^e	
	AAG 0.5	–0.003 ^{bc}		4.60 ^d		0.79 ^{abc}		0.05 ^e	
	FG 0.1	–0.004 ^c		2.70 ^d		0.75 ^{abc}		0.00 ^e	
	FG 0.5	–0.008 ^c		3.27 ^d		0.65 ^{abc}		0.10 ^e	
WPI	No gum	–0.007 ^c		0.00 ^d		0.19 ^c		0.29 ^e	
	AAG 0.1	–0.008 ^c		3.00 ^d		0.87 ^{abc}		Nd	
	AAG 0.5	–0.003 ^{bc}		7.53 ^d		1.21 ^{abc}		0.10 ^e	
	FG 0.1	–0.005 ^c		2.30 ^d		0.83 ^{abc}		Nd	
	FG 0.5	–0.003 ^{bc}		4.91 ^d		1.14 ^{abc}		0.00 ^e	

^{a–h}Different letters between the cryogels denote a significant difference (p < 0.05) among the cryogels for the same column to Tukey’s post hoc means comparison test. ¹first-order kinetics. ²Weibull’ model parameters. Nd: not detected.

higher content in peptides with high free radical scavenging performance (Ries, Ye, Haisman, & Singh, 2010; X. Yin et al., 2022).

In most of the cases, the incorporation of soluble dietary fibre aims at the creation of physicochemical barriers against to commonly encountered physicochemical stressors. Except for NaCas–PSG systems, the inclusion of the gums did not offer any tangible cell preservation benefits. Previous studies have shown that preservation performance of polysaccharides is species and strain dependent. In view of this, Peredo, Beristain, Pascual, Azuara, and Jimenez (2016) demonstrated that the inclusion of biopolymers such as psyllium, potato starch or inulin were more efficient in protecting *L. plantarum* than *L. casei Shirota* over a 30 days storage at 4 and 22 °C. On the other hand, the inclusion of rice bran fibres in freeze-dried ionotropically crosslinked pectin capsules preserved better the biological activity of *L. acidophilus* than Hi-maize starch and inulin (Raddatz et al., 2020).

To estimate the shelf-life of the probiotic cryogels, the minimum total load in viable probiotic cells according to the recommendation of

Table 2
Estimated cryogels shelf-life (in days) cryogels influenced by gum type and content and storage conditions.

Protein	Gum	¹ a _w 0.11	² a _w 0.11	² a _w 0.11	² a _w 0.75
		5 °C	20 °C	37 °C	20 °C
NaCas	No gum	>3 years ^{bc}	141 ^{defg}	10 ^c	13 ^e
	AAG 0.1	>3 years ^{ab}	162 ^{cdefg}	15 ^b	10 ^{sh}
	AAG 0.5	>3 years ^{bc}	213 ^{bcde}	16 ^b	21 ^b
	FG 0.1	>3 years ^a	195 ^{bcdef}	16 ^b	9 ^{gh}
	FG 0.5	>3 years ^{abc}	252 ^{bcd}	26 ^a	24 ^a
N1:1 W	No gum	>3 years ^c	302 ^{ab}	14 ^b	18 ^{cd}
	AAG 0.1	>3 years ^{bc}	271 ^{bc}	6 ^d	18 ^{cd}
	AAG 0.5	>3 years ^{bc}	77 ^{fg}	6 ^d	17 ^d
	FG 0.1	942 ^c	51 ^g	<2 ^f	12 ^{ef}
	FG 0.5	512 ^c	97 ^{efg}	7 ^d	17 ^d
WPI	No gum	516 ^c	388 ^a	6 ^d	20 ^{bc}
	AAG 0.1	506 ^c	37 ^g	<2 ^f	8 ^h
	AAG 0.5	>3 years ^{bc}	45 ^g	3 ^e	13 ^{ef}
	FG 0.1	904 ^c	33 ^g	<2 ^f	9 ^{gh}
	FG 0.5	>3 years ^{bc}	33 ^g	<2 ^f	11 ^{fg}

^{a–g}Different letters between the cryogels denote a significant difference (p < 0.05) among the cryogels for the same column to Tukey’s post hoc means comparison test. The effect of the temperature and physical state was significant for all the tested cryogels. The shelf-life was estimated as the maximum storage time with LGG counts of at least 6 logCFU.g⁻¹. ¹Shelf life estimated by first order kinetics. ²shelf life estimated by Weibull’ model.

FAO/WHO (FAO/WHO, 2002), i.e. 6 logCFU g⁻¹ was used as a boundary. As shown in Table 2, the shelf-life of the probiotic cryogels at chilling storage conditions ranged from 1.4 to more than 3 years, which is compliant with the standards of commercial anhydrobiotic formulations (Kieps & Dembczyński, 2022). As expected, the shelf-life of the probiotic cryogels was steeply declined when extrinsic physicochemical stressors were imposed, i.e. t_{shelf-life} = 2–388 days.

3.3. Colloidal changes of the cryogels and viability of *Lactocaseibacillus rhamnosus* GG throughout in vitro digestion

The assessment of the colloidal responsiveness of the cell-conveying matrix to the gastrointestinal environment is crucial for understanding its bioactive potential (de Melo Pereira et al., 2018; Sanders & Marco, 2010). The model boluses were prepared by mixing one cryogel monolith with the appropriate amount of artificial saliva at 50 s⁻¹ without any mechanical crushing (e.g. processing in an artificial mouth or Stomacher) of the matrix throughout the simulating oral processing. Therefore, the amount of the released free LGG cells was extremely restricted. Then, the partially swollen cryogel boluses were mixed with the simulating gastric fluids and allowed to incubate for 2 h. As shown in the Suppl. Fig. 1, at the end of in vitro gastric processing, the cryogel matrices, particularly those based on NaCas, underwent limited disintegration. Furthermore, the presence of PSGs, especially at 0.5% wt., was found to impede the disintegration of the swollen cryogels, with AAG being more effective than FG. To gain insight into the mean size of the residual particles in the gastric chymes, after the removal of the intact swollen cryogels, at least five CLSM micrographs were analysed by using ImageJ software and the Feret’s diameters (D_f) were calculated. As shown in Fig. 5, the gastric chymes of the WPI-based cryogels comprised the largest particles (i.e. D_f = 9–204 μm), compared to the mixed protein and NaCas-based exemplars (i.e. D_f = 9–133 μm and 4–37 μm, respectively). This finding corroborates our previous research on the water disintegration behaviour of milk protein-based cryogels (Hellebois et al., 2023). The inclusion of PSGs in the NaCas-based cryogels resulted in an increase in the particles’ mean size proportionally to the gum content. In a recent study, we have demonstrated that the presence of AAG and FG prolonged the water disintegration time of NaCas cryogels due to the ability of the gums to reinforce the skeleton of the cryogels (Hellebois, Addiego, et al., 2024). On the other hand, the presence of the PSGs in the mixed protein and WPI based cryogels reduced the mean size of the residual particles in a reciprocal to the gum

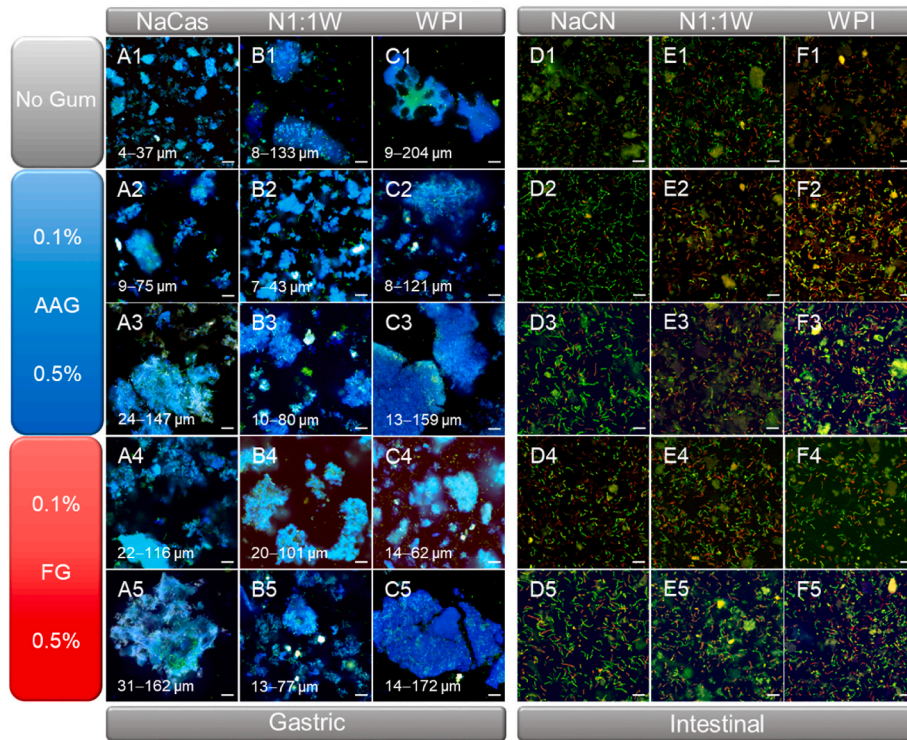


Fig. 5. CLSM acquired micrographs of gastric (A–C) and intestinal (E–F) chymes of the milk protein-based cryogels in the presence of alfalfa and flaxseed gum at 0 (1), 0.1 (2 & 4) and 0.5% wt. (3 & 5). Scale bar: 20 μm . Proteins are stained in blue (Fast Green, $\lambda\text{Ex} = 633 \text{ nm}$, $\lambda\text{Em} = 635\text{--}680 \text{ nm}$), live bacteria in green (Syto9, $\lambda\text{Ex} = 488 \text{ nm}$, $\lambda\text{Em} = 498\text{--}550 \text{ nm}$) and inactivated bacteria in red (propidium iodide, $\lambda\text{Ex} = 488 \text{ nm}$, $\lambda\text{Em} = 585\text{--}640 \text{ nm}$). NaCas: Sodium Caseinate, WPI: Whey Protein, N1:1 W: binary mixture of NaCas and WPI protein at 1:1 ratio.

content fashion. Nonetheless, no clear association of the D_f values with the microstructural (e.g. porosity, vessels thickness) and physicochemical (e.g. bulk density, shrinkage, disintegration time, etc.) aspects of the cryogels was found. It should be noted that in all cases the CLSM micrographs confirmed the cryogels' ability to prevent the uncontrolled release of free LGG cells in the continuous gastric fluid phase (as indicated by the SYTO9 fluorophore-stained living cells), and thus, diminishing the lethal effects of the harsh gastric environment conditions. Indeed, as illustrated in Fig. 6, a very good protection of the viability of

the LGG cells in the gastric chymes was observed, i.e. 9.80 vs. 9.45 $\log\text{CFU}\cdot\text{g}^{-1}$, for initial matrix (cryogels stored at 5 $^{\circ}\text{C}$ for 60 days) and gastric chymes, respectively. In all cases, the embedment of LGG cells into the cryogel scaffold offered a substantial protection against gastric fluids compared to the free (non-encapsulated) LGG cells (Fig. 6) Nevertheless, the survivability of LGG under in vitro gastric conditions was predominantly influenced by the protein composition ($p < 0.001$) rather than the PSG type and content ($p > 0.05$). In agreement with our previous findings (Hellebois, Canel, et al., 2024), the LGG cell

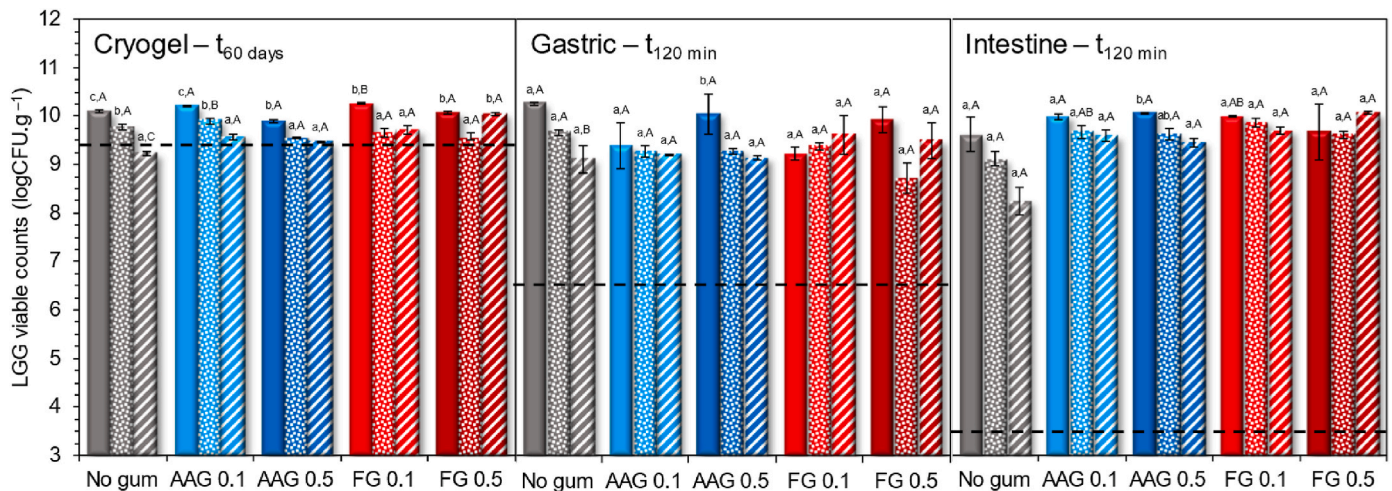


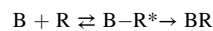
Fig. 6. LGG cells viability throughout the static in vitro simulated digestion following the INFOGEST protocol embedded in sodium caseinate (NaCas, plain bars), mixed sodium caseinate – whey protein isolate at 1:1 ratio (N1:1 W, dotted bars) and whey protein isolate (WPI, dashed bars) protein-based cryogels influenced by the presence of alfalfa (AAG) or flaxseed (FG) gums at either 0.1 or 0.5% wt. Dashed lines represents the LGG viable counts in non-encapsulated bacteria systems for each digestive step. ^{A–B,C}Different letters among the digestive steps for the same cryogel (uppercase) and at each digestive steps among the three protein composition (lowercase) denotes significant ($p < 0.05$) differences.

preserving capacity throughout gastric processing was proportional to the increase in the NaCas content. The protective role of soluble dietary fibres lies in their capability to protect the viability of probiotics in protein-rich freeze-dried or spray-dried particulates arising from their ability to reduce the rate of gastric fluids diffusion into the protein scaffold, thus enhancing the acid resistance of the encapsulated cells (Desmond, Ross, O'Callaghan, Fitzgerald, & Stanton, 2002; Yao, Liu, He, Hu, & Liu, 2023). Moreover, the dense structure of the pre-coagulated milk proteins, coupled with their buffering capacity, has been previously demonstrated to improve the survivability of probiotics by maintaining a higher pH within the core material (Heidebach, Först, & Kulozik, 2009). The presence of residual glucose may also enhance the viability of LGG under gastric conditions. Prior research has indicated that the presence of metabolisable sugars, such as glucose, enables LGG to produce sufficient quantities of adenosine triphosphate (ATP), necessary for the extrusion of H^+ protons from their cytosol via the F_0F_1 -ATPase, which improves LGG survivability in acidic conditions (Corcoran, Stanton, Fitzgerald, & Ross, 2005). The observed minor effects of the polysaccharides on the gastric survivability of LGG are likely due to their relatively low concentration compared to the milk proteins and sugars.

On admixing with the intestinal fluids, a complete disintegration of the cryogel matrices leading to a burst release of the LGG cells was observed (Suppl. Fig. 1), confirming their feasibility as alternative scaffolds for targeted release of probiotics. As illustrated in the CLSM micrographs (Fig. 5) and TVCs (Fig. 6), the bile salt and pancreases induced cellular stress was reduced proportionally to the NaCas to WPI mass ratio (9.87, 9.58, 9.41 for NaCas, N1:1 W, and WPI, respectively). Nonetheless, the TVCs in the intestinal digesta were slightly higher than those determined in the gastric chymes (ranging from 0.1 to 0.26 $\log CFU.g^{-1}$), implying that in all cases the stressed LGG cells were still cultivable. On the other hand, the free (non-encapsulated) LGG cells experienced an approx. 3 $\log CFU.g^{-1}$ reduction in the TVCs suggesting the bile salt sensitivity of LGG at physiologically relevant concentrations. Stemming from their surface-active and amphipathic properties, bile salts can disrupt the bacterial cell membrane's lipid bilayer causing cytoplasmic leakage and damage the intracellular proteins and DNA (Mendonça et al., 2023; Ventura et al., 2011). In accordance with the findings of Giulio et al. (2005), the presence of trehalose and glucose was associated with a significant improvement of the bile salt tolerance of LGG. In addition, the presence of proteins in the wall material may suppress the bile salt induced cellular injuries due to their capacity to serve as a protective barrier between the bile salts and the phospholipid bilayer (Vargas, Olson, & Aryana, 2015).

3.4. Adhesion of LGG to an *in vitro* gut epithelium model

Although the preservation of the biological activity of probiotics throughout gastrointestinal transit is an essential aspect of an effective encapsulation strategy, promoting the ability of the living cells to adhere to the mucus layer of the intestinal epithelium should be rigorously evaluated (de Melo Pereira et al., 2018; Sanders & Marco, 2010). To assess the ability of the cryogels to promote the LGG cells adhesion a mucin producing co-culture model (Caco-2/HT-29) of the gut epithelium was employed. As clearly depicted in the representative SEM and CLSM micrographs, a satisfactory amount of predominantly living LGG cells was adhered to the mucus-rich microdomains of the co-culture model (Fig. 7). According to the microbial enumeration of the mechanically disrupted epithelial tissues (Fig. 8), the LGG bacterial densities ranged from 2.24 to 4.71 $\log CFU.cm^{-2}$, with the highest amount of culturable LGG cells being detected in the NaCas-based digesta (4.56 vs. 4.18 and 4.01 $\log CFU.cm^{-2}$, for NaCas, N1:1 W and WPI, respectively). Worth to note that in the case of the N1:1 W and WPI systems, the presence of PSG significantly enhanced the LGG adhesion properties. Overall, FG exhibited a better LGG adhesion promoting ability compared to AAG i.e. 4.55 vs 4.26 $\log CFU.cm^{-2}$, respectively. On the other hand, the presence of AAG in the NaCas based digesta did not significantly modify the LGG adhesion properties. In all cases, the inclusion of PSG at a concentration as low as 0.1% wt. was sufficient to enhance the LGG mucoadhesion. It is established that the adhesion of the probiotic cells to the gut mucosa is initiated by weak and reversible hydrophobic binding interactions and in a later stage through specific adhesins – mucins interactions (Bron, Van Baarlen, & Kleerebezem, 2012; Han et al., 2021) represented as follows:



Where B is the bacterial concentration, R is the constant number of monolayer cell receptor sites, $B-R^*$ represents the unstable intermediate complex (formed via weak physical interactions) and BR is the stable adhesin – mucin complex. As illustrated in Fig. 8 the number of LGG cells adhered onto the mucus layer of the co-culture model was highly dependent on the LGG TVCs in the intestinal digesta ($r = 0.88$, $p < 0.001$), indicating the probabilistic character of the cell adhesion phenomena. To get a deeper insight these data were fitted to the Hill's model (Eq. (5)):

$$BR = R_{\max} \frac{B^n}{k^n + B^n} \quad (5)$$

where B and BR denote the viable cells present in the intestinal digesta

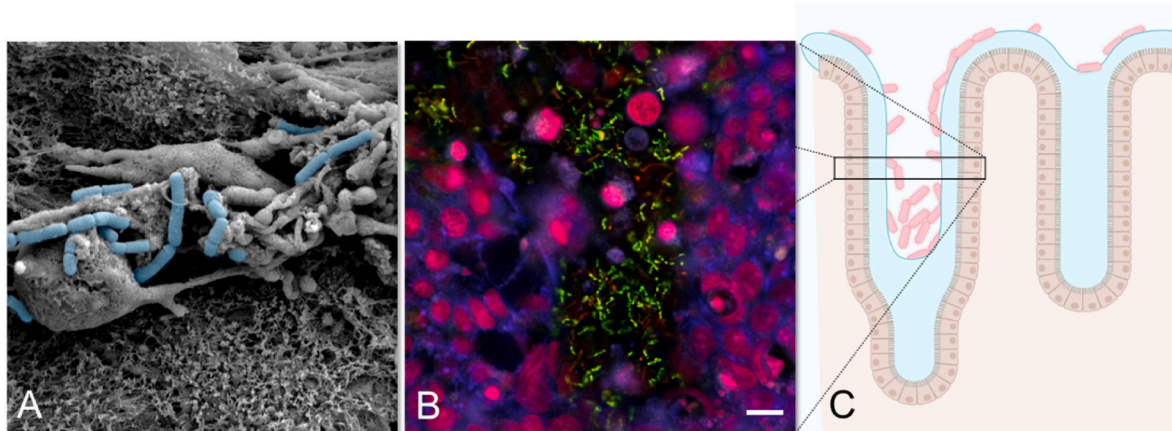


Fig. 7. Representative SEM (A) and CLSM (B) micrographs of Caco2/HT29 coculture model after 120 min of incubation in the presence of intestine chymes of digested and the proposed adhesion mechanism (C). Scale of the micrographs: SEM $17 \times 17 \mu m^2$, CLSM $140 \times 140 \mu m^2$. SEM micrograph blue colour: LGG cells. CLSM micrograph stains: green (Syto9): living LGG cells, red (propidium iodide): inactivated LGG and epithelial cells, blue (fast green): glycoprotein of the mucosa.

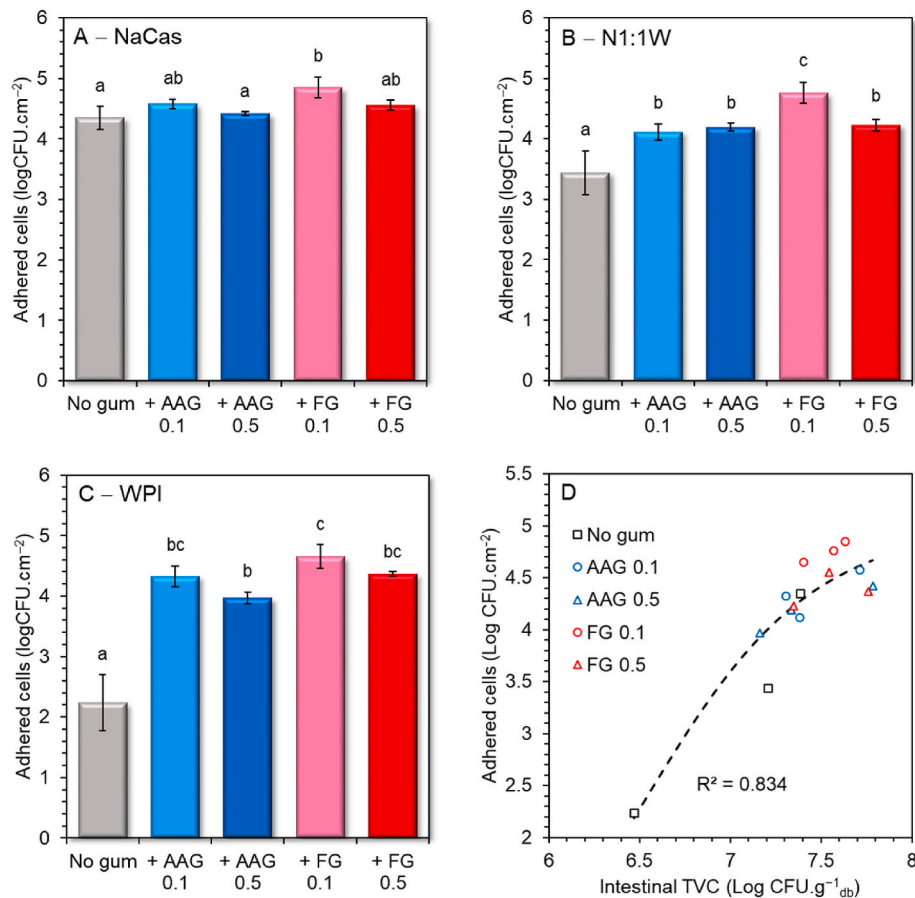


Fig. 8. Number of adhered cultivable LGG cells to the Caco2/HT29 coculture model (expressed in logCFU.cm⁻²) from digested sodium caseinate (NaCas, A), mixed protein with NaCas:WPI ratio of 1:1 (N1:1 W, B) and whey protein isolate (WPI, C)-based cryogels. The relationship between the number of adhered cells and the TVC in the intestinal fluids ($t = 120$ min) is displayed in D. The dashed line (D) represent the Hill model fitted to the data. AAG 0.1 and AAG 0.5, alfalfa gum at 0.1 and 0.5% wt., respectively. FG 0.1 and FG 0.5, flaxseed gum at 0.1 and 0.5% wt., respectively. ^{a-c}Different letters between the samples denote a significant difference ($p < 0.05$) according to Tukey's post hoc means comparison test.

and adhered onto the mucosa layer, respectively, n is the cooperativity constant, R_{max} is the maximum number of viable LGG cell that can be adhered to the mucosa layer and k denotes the amount LGG cells required to achieve $\frac{R_{max}}{2}$ (Mays, Chappell, & Nair, 2020). The cooperativity constant was estimated at $n = 14.9$, suggesting that once a bacterial cell is specifically adhered to the mucins its affinity to intercellular homophilic interactions, i.e. pili – pili hydrophobic bonding, is increased (Tripathi et al., 2013). The maximum adherence capacity was estimated at $R_{max} = 5.1$ logCFU.cm⁻² confirming that the presence of PSGs was crucial for maximising the LGG adhesion capacity. Although the exact mechanism of action of the PSGs needs to be further investigated, we assume that their presence in the microbe – mucus interface mediates the non-specific microbe – mucin interactions. It is also hypothesised that the presence of carboxyl groups in FG (contrary to AAG) explain the higher adherence capacity of the former. In line with these hypotheses, Liu et al. (2020) demonstrated that the grafting of side functional groups e.g., –COOH or –SH (via TEMPO oxidation and amide reaction) to konjac glucomannan enhanced the adhesin – mucin interactions via non-specific (e.g., hydrogen bonds, van der Waals forces) and disulfide bonding, respectively.

3.5. Proteomic characterisation of the gastric and intestinal phases

As clearly illustrated in the capillary SDS-PAGE electropherograms of the cryogel gastric phases (Fig. 9), the intensity of the characteristic bands associated with the presence of total (α_{s1} –, β –, and κ –) caseins, β -lactoglobulin and α -lactalbumin was increased proportionally to the

increase in the $m_{NaCas/WPI}$. Although native β -lactoglobulin is highly resistant to pepsinolysis, the presence of a broad peptide band at 10 kDa indicated the partial cleavage of the whey protein during gastric processing. This is mainly attributed to the denaturation of whey proteins during the heat treatment of the cryogel precursors (Barbé et al., 2013). The addition of PSGs promoted the pepsin induced cleavage of the proteins though only in the case of the FG stabilised cryogels it was possible to detect a dose dependent effect. In this context, the NaCas containing systems showed a higher resistance to pepsinolysis at 0.5% wt. FG, whilst an adverse effect was observed in the WPI-based exemplars. Our findings align with the observations of Markussen, Madsen, Young, and Corredig (2021) who reported that contrary to galactomannans (guar gum), anionic polysaccharides (sodium alginate and pectin) delayed the in vitro gastric peptic cleavage of the caseins fraction of milk protein concentrate. A good correlation between the pepsin induced cleavage of the proteins and the disintegration profile of the cryogels was found. As we have previously demonstrated (Hellebois, Canuel, et al., 2024), the presence of 0.5% FG in the NaCas and N1:1 W cryogels resulted in slower disintegration rates ($\tau = 521, 138, 65$ s, for NaCas, N1:1 W and WPI, respectively) and larger residual particles ($D_{[4, 3]} = 94, 150, 63$ μ m for NaCas, N1:1 W and WPI, respectively) than WPI, inhibiting sterically the progress of pepsinolysis. The opposite effect was observed in the case of WPI cryogels containing 0.1% FG. In accordance to our previous work (Hellebois, Canuel, et al., 2024), the exposure of the gastric phases to the pancreases induced a complete cleavage of the proteins and polypeptides (>6500 Da).

To gain insight into any potential secondary health benefit

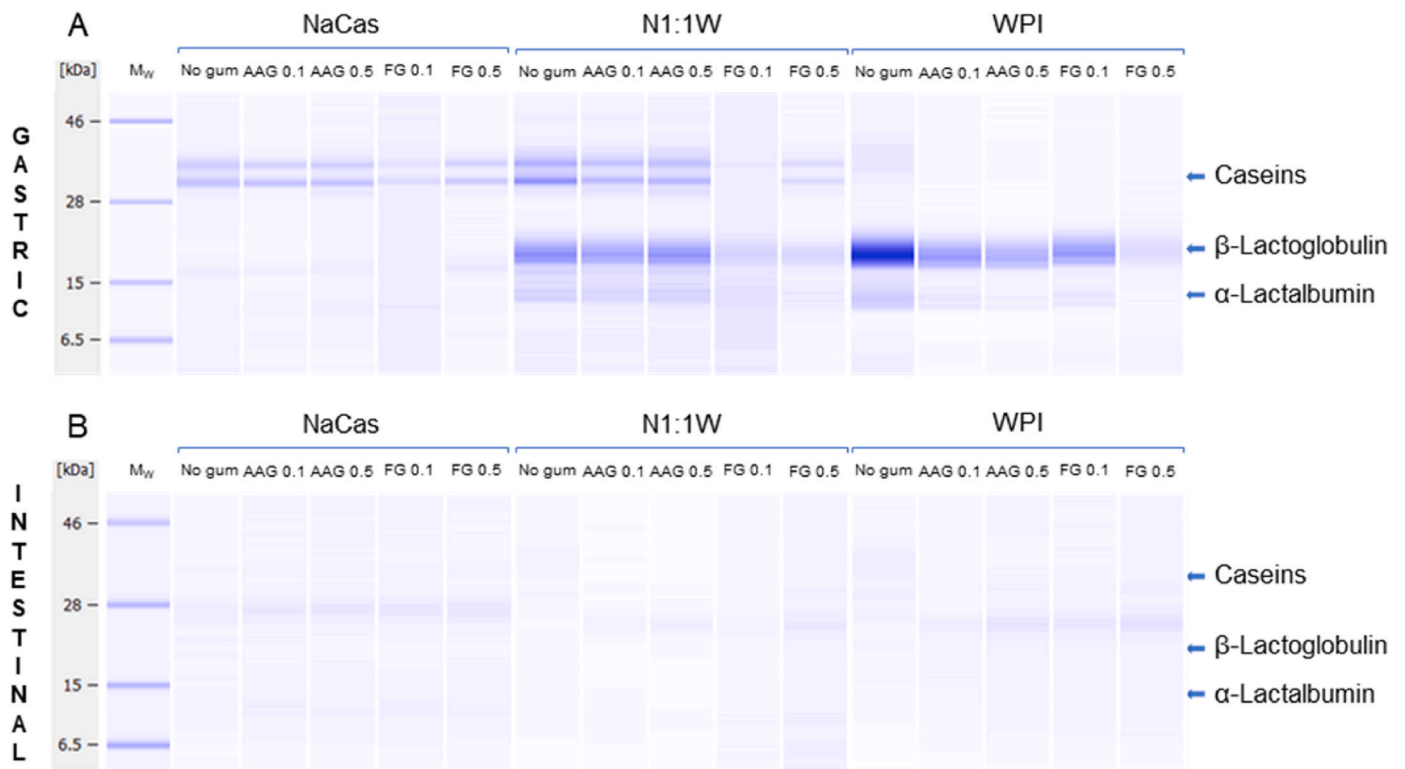


Fig. 9. Capillary SDS-PAGE electropherograms of the gastric (A) (tgastric = 120 min) and intestinal (B) (tintestinal = 120 min) milk protein cryogel digesta as influenced by the protein type (sodium caseinate, NaCas; whey protein, WPI; mixed NaCas:WPI at a ratio of 1:1, N1:1 W), gum type (alfalfa gum, AAG; flaxseed gum, FG) at 0.1 and 0.5% wt.

conferring effects, the peptidome (500–3000 Da) of the intestinal digesta was analysed using nano-LC-MS. As shown in Fig. 10 the intestinal digesta contained peptides composed of 6–24 amino acids, following a Gaussian distribution with a median of 9–11 depending on the cryogel composition, in agreement with our previous study (Hellebois, Canuel, et al., 2024). The prevalence of long-chain (i.e. > 17) peptides was adversely correlated to the $m_{\text{NaCas/WPI}}$. Interestingly, the presence of PSGs in the intestinal digesta was associated with release of low to intermediate chain peptides, i.e. < 11 (Fig. 10 A). On the contrary the presence of PSGs in the mixed protein and WPI digesta did not affect in a straightforward fashion the peptides length distribution pattern.

As regards the protein origin of the release peptides (Fig. 11), the prevalence of peptides per protein class was not only associated with the protein composition of the cryogels but also with the PSG type and content. As well depicted in Fig. 11, the PSGs did not remarkably modified the peptidome composition, with most of the identified peptides being originated from β -Lg and α -La. On the contrary, the peptidomes of the intestinal digesta of the NaCas cryogels containing 0.1% wt. PSG, showed higher affinity to their non-stabilised NaCas counterparts. The increase of the PSG content in the intestinal digesta of the NaCas cryogels resulted in a significant reduction in number of the peptides originating from β -, α _{s1}- and κ -caseins yet without impacting those stemming from whey proteins. In a similar fashion, the presence of PSGs in the mixed protein cryogel intestinal digesta resulted in a proportional to their content decrease in the abundance of β -Lg and α -La derived peptides.

As shown in Table 3, a total of 14 bioactive peptides were at least one aliquot of intestinal digesta. Two bioactive peptides originating from β -Lg, i.e. ⁵⁹VEELKPTPEGDL⁷³ and ¹⁴¹TPEVDDEALEK¹⁵¹ associated with zinc binding (Udechukwu, Dang, & Udenigwe, 2021) and DPP-IV inhibitory (Power, Fernández, Norris, Riera, & FitzGerald, 2014) activities were detected in all intestinal digesta indicating their high resistance to pancreases. Noteworthy, the ¹⁴¹TPEVDDEALEK¹⁵¹ (IC₅₀ =

320 μ M) was the most abundant bioactive amino acid sequence amounting to 10–15% of the total peptides detected. Three bioactive peptides, i.e. ¹³⁸VRTPEVDDE¹⁴, ⁵⁸YVEELKPTPEGDL⁷⁰, ¹⁹⁵SDIPNPIGSENSEK²⁰⁸ and ⁶²LKPTPEGDL⁷⁰ (IC₅₀ = 45 μ M), associated with zinc binding (Udechukwu et al., 2021), antioxidant (Basilicata et al., 2018), and antimicrobial (Hayes, Ross, Fitzgerald, Hill, & Stanton, 2006) properties, were persistently detected in the mixed protein and WPI based intestinal phases. On the other hand, the ⁹⁹EDVPSE¹⁰⁵ and ¹⁹⁵SDIPNPIGSE²⁰⁴ amino acid sequences, documented for their osteoanabolic (Reddi, Shanmugam, Tanedjeu, Kapila, & Kapila, 2018) and antidiabetic (Gong et al., 2020) potential, were primarily identified in the NaCas-based cryogel derived intestinal phases. Interestingly, the ¹⁴⁸LHLPLP¹⁵⁴ (IC₅₀ = 425 μ M) amino acid sequence exerting an ACE-binding activity – known for its high resistance to pancreases due to the presence of branched amino acids (leucine) and – was the less prevalent in the intestinal digesta. It is hypothesised that the ¹⁴⁸LHLPLP¹⁵⁴ was further cleaved to more pancreases-resistant amino acid sequences, i.e. ¹⁵⁰LPLP¹⁵³ (IC₅₀ = 720 μ M) and ¹⁴⁹HLPLP¹⁵³ (IC₅₀ = 41 μ M), which could not be detected due to the minimum peptide length cut-off of the implemented analytical protocol. Ultimately, it should be highlighted that the PSG type and concentration did not create any clear peptidome patterns and hence, the protein composition of the cryogels is the major driver of the secondary bioactive potential.

4. Conclusions

In the present work, the feasibility of protein–plant seed gum cryogels as alternative xero-scaffolds embedding living probiotic cells was assessed. The protein type was found to be the most critical parameter for achieving maximal LGG survivability during the xero-structuration, storage, and in vitro gastrointestinal digestion. Sodium caseinate was clearly associated with an enhanced lyoprotective ability compared to WPI, due to its efficacy to retain water in the vicinity of the polar

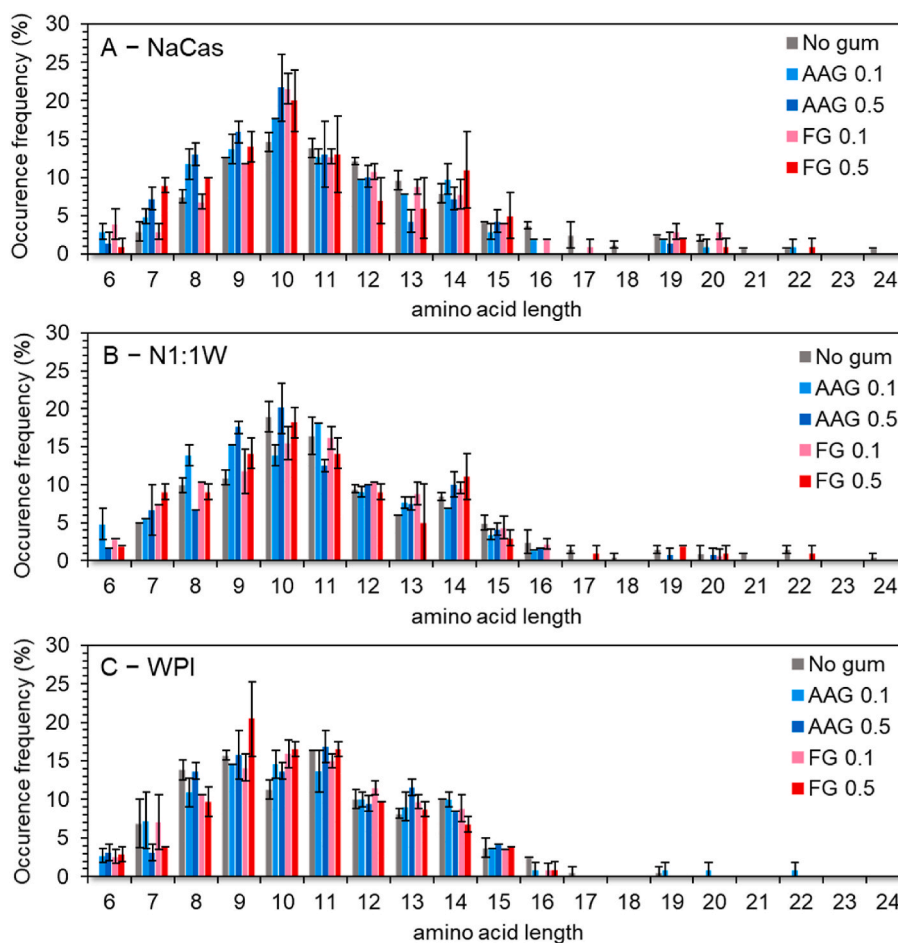


Fig. 10. Milk protein originating peptide sequences length from NaCas (A), N1:1 W (B) and WPI (C) cryogels in the intestinal chymes influenced by the protein type (sodium caseinate, NaCas; whey protein, WPI; mixed NaCas:WPI at a ratio of 1:1, N1:1 W), and the presence of PSGs (alfalfa gum, AAG; flaxseed gum, FG) at 0.1 and 0.5% wt.

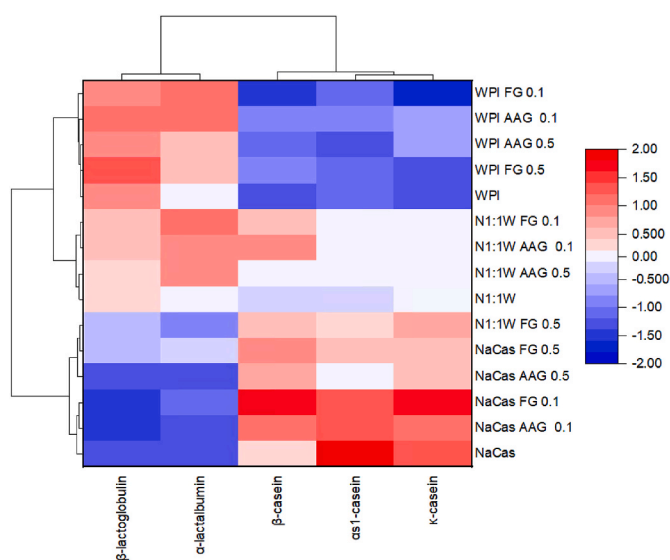


Fig. 11. Heat-map with dendrogram analysis of the effect of the addition of alfalfa (AAG) or flaxseed (FG) gums at either 0.1 or 0.5% on the prevalence of milk protein to produced detectable peptides sequences in the intestinal chymes of the cryogels. NaCas: Sodium Caseinate (A), WPI: Whey Protein Isolate (C), N1:1 W denote mixed protein system of NaCas:WPI ratio of 1:1 (B).

phospholipid bilayer interface during the desiccation process. In a similar fashion, NaCas was able to preserve maximally the biological activity of LGG throughout controlled storage by preventing the undesirable changes in the structural integrity of the LGG cell membranes due to physical state and biochemical alterations. As expected, the LGG inactivation rates were significantly higher at elevated temperature (37 °C) and relative humidity conditions (75% RH). The presence of PSG had minor effects on the LGG survival during the desiccation process but mixed effects on the inactivation rates of LGG were observed depending on the protein composition of the cryogels. In most cases, the cryogels exhibited a low degree of disintegration and in vitro digestibility in the gastric fluids allowing a high LGG cell protection in the highly acid gastric environment. On the other hand, the exposure of the gastric chymes into the pancreases resulted in a burst release of living LGG cells and bioactive peptides behaviour. Although the LGG bioadhesion properties were ameliorated in the NaCas based intestinal digesta, the presence of PSG and particularly flaxseed gum was identified as a key factor in achieving a maximal load of viable LGG cells adhered to the mucus layer of the gut epithelium model. Our study confirmed that cryogels are promising and easily tuneable xero-templates for targeted delivery of probiotics.

CRedit authorship contribution statement

Thierry Hellebois: Conceptualization, Formal analysis, Investigation, Writing – original draft, Writing – review & editing. **Jennyfer Fortuin:** Formal analysis, Investigation, Writing – review & editing.

Table 3
Bioactive peptide sequences derived from milk protein after in vitro intestinal digestion of cryogels: Influence of gum type and content.

¹ Bioactive peptide sequence	Protein	² Bioactivity (IC ₅₀ μM)	NaCas					N1:1 W					WPI					
			No gum	AAG 0.1	AAG 0.5	FG 0.1	FG 0.5	No gum	AAG 0.1	AAG 0.5	FG 0.1	FG 0.5	No gum	AAG 0.1	AAG 0.5	FG 0.1	FG 0.5	
⁹⁹ EDVPSE ¹⁰⁵	αs1-cn	^a Osteoanabolic	✓	✓	✓	✓	✓		✓			✓	✓		✓			
⁵⁰ EKVNELSK ⁵⁶	αs1-cn	^b ACE-inhibitory (5998)	✓															
³⁸ FFVAPFPEVFGK ⁴⁹	αs1-cn	^c ACE-inhibitory (18)	✓															
¹⁹⁵ SDIPNPIGSENSEK ²⁰⁸	αs1-cn	^d Antimicrobial	✓				✓	✓			✓	✓	✓	✓	✓			✓
¹⁹⁵ SDIPNPIGSE ²⁰⁴	αs1-cn	^e Antidiabetic	✓	✓	✓		✓	✓		✓								
¹⁶⁰ HQPHQPLPPTVMFPPQ ¹⁷⁵	β-cn	^f Zinc binding	✓															
¹⁴⁸ LHLPLPL ¹⁵⁴	β-cn	^g ACE-inhibitory (433)						✓						✓				
⁶² LKPTPEGDL ⁷⁰	β-Lg	^h DPP-IV Inhibitory (45)						✓	✓	✓	✓	✓	✓	✓		✓		✓
⁵⁹ VEELKPTPEGDL ⁷³	β-Lg	^f Zinc binding	✓	✓	✓		✓	✓	✓	✓	✓	✓	✓	✓	✓	✓	✓	✓
⁵⁸ VVEELKPTPEGDL ⁷⁰	β-Lg	ⁱ Antioxidant	✓				✓	✓	✓	✓	✓	✓	✓	✓	✓	✓	✓	✓
²⁶ LDIQKVAGTW ³⁵	β-Lg	^j ACE-inhibitory (21)						✓										
¹⁴¹ TPEVDDEALEK ¹⁵¹	β-Lg	^k DPP-IV Inhibitory (320)	✓	✓	✓		✓	✓	✓	✓	✓	✓	✓	✓	✓	✓	✓	✓
¹³⁸ VRTPEVDDE ¹⁴⁷	β-Lg	^f Zinc binding					✓		✓	✓	✓	✓	✓	✓	✓	✓	✓	✓
¹⁰⁸ VVLVLDTDYK ¹¹⁶	β-Lg	^l DPP-IV Inhibitory (424)	✓				✓	✓		✓	✓	✓	✓	✓				✓

¹ Peptide sequence loci were determined using UniProt protein sequences.

² References for the peptides bioactivities.

^a (Reddi et al., 2018).

^b (Tu et al., 2018).

^c (Tauzin, Miclo, & Gaillard, 2002).

^d (Hayes et al., 2006).

^e (Gong et al., 2020).

^f (Udechukwu et al., 2021).

^g (Quirós et al., 2007; Robert, Razaname, Mutter, & Juillerat, 2004).

^h (Lacroix & Li-Chan, 2014).

ⁱ (Basilicata et al., 2018).

^j (Lacroix, Meng, Cheung, & Li-Chan, 2016).

^k (Power et al., 2014).

^l (Silveira, Martínez-Maqueda, Recio, & Hernández-Ledesma, 2013).

Sébastien Cambier: Formal analysis, Investigation, **W. Servane Conantal:** Investigation. **Céline C. Leclercq:** Formal analysis, Investigation, Writing – review & editing. **Claire Gaiani:** Conceptualization, Supervision, Writing – review & editing. **Christos Soukoulis:** Conceptualization, Funding acquisition, Project administration, Supervision, Writing – review & editing.

Declaration of competing interest

The authors declare that they have no known competing financial interests or personal relationships that could have appeared to influence the work reported in this paper.

Data availability

Data will be made available on request.

Acknowledgements

This work was supported by the Luxembourg National Research Fund, FNR (Project PROCEED: CORE/2018/SR/12675439). The authors would like to acknowledge Manon Hiolle (Ingredia, Arras, France) for providing the WPI.

Appendix A. Supplementary data

Supplementary data to this article can be found online at <https://doi.org/10.1016/j.foodhyd.2024.109867>.

References

- Aschenbrenner, M., Foerst, P., & Kulozik, U. (2015). Freeze-drying of probiotics. In *Advances in probiotic technology*. CRC Press.
- Barbé, F., Ménard, O., Le Gouar, Y., Buffière, C., Famelart, M.-H., Laroche, B., et al. (2013). The heat treatment and the gelation are strong determinants of the kinetics of milk proteins digestion and of the peripheral availability of amino acids. *Food Chemistry*, 136(3), 1203–1212. <https://doi.org/10.1016/j.foodchem.2012.09.022>
- Basilicata, M. G., Pepe, G., Adesso, S., Ostacolo, C., Sala, M., Sommella, E., et al. (2018). Antioxidant properties of buffalo-milk dairy products: A β -lg peptide released after gastrointestinal digestion of Buffalo ricotta cheese reduces oxidative stress in intestinal epithelial cells. *International Journal of Molecular Sciences*, 19(7). <https://doi.org/10.3390/ijms19071955>. Article 7.
- Brodtkorb, A., Egger, L., Alminger, M., Alvito, P., Assunção, R., Ballance, S., et al. (2019). INFOGEST static in vitro simulation of gastrointestinal food digestion. *Nature Protocols*, 14(4), 991–1014. <https://doi.org/10.1038/s41596-018-0119-1>
- Bron, P. A., Van Baaren, P., & Kleerebezem, M. (2012). Emerging molecular insights into the interaction between probiotics and the host intestinal mucosa. *Nature Reviews Microbiology*, 10(1), 66–78. <https://doi.org/10.1038/nrmicro2690>
- Burgain, J., Corgneau, M., Scher, J., & Gaiani, C. (2015). Chapter 20—encapsulation of probiotics in milk protein microcapsules. In L. M. C. Sagis (Ed.), *Microencapsulation and microspheres for food applications* (pp. 391–406). Academic Press. <https://doi.org/10.1016/B978-0-12-800350-3.00019-4>.
- Burgain, J., Gaiani, C., Cailliez-Grimal, C., Jeandel, C., & Scher, J. (2013). Encapsulation of *Lactobacillus rhamnosus* GG in microparticles: Influence of casein to whey protein ratio on bacterial survival during digestion. *Innovative Food Science & Emerging Technologies*, 19, 233–242. <https://doi.org/10.1016/j.ifset.2013.04.012>
- Cakmak, H., Ilyasoglu-Buyukkestelli, H., Sogut, E., Ozyurt, V. H., Gumus-Bonacina, C. E., & Simsek, S. (2023). A review on recent advances of plant mucilages and their applications in food industry: Extraction, functional properties and health benefits. *Food Hydrocolloids for Health*, 3, Article 100131. <https://doi.org/10.1016/j.fhfh.2023.100131>
- Cook, M. T., Tzortzis, G., Charalampopoulos, D., & Khutoryanskiy, V. V. (2012). Microencapsulation of probiotics for gastrointestinal delivery. *Journal of Controlled Release*, 162(1), 56–67. <https://doi.org/10.1016/j.jconrel.2012.06.003>
- Corcoran, B. M., Stanton, C., Fitzgerald, G. F., & Ross, R. P. (2005). Survival of probiotic lactobacilli in acidic environments is enhanced in the presence of metabolizable sugars. *Applied and Environmental Microbiology*, 71(6), 3060–3067. <https://doi.org/10.1128/AEM.71.6.3060-3067.2005>
- de Melo Pereira, G. V., de Oliveira Coelho, B., Magalhães Júnior, A. I., Thomaz-Soccol, V., & Soccol, C. R. (2018). How to select a probiotic? A review and update of methods and criteria. *Biotechnology Advances*, 36(8), 2060–2076. <https://doi.org/10.1016/j.biotechadv.2018.09.003>
- Desmond, C., Ross, R. P., O'Callaghan, E., Fitzgerald, G., & Stanton, C. (2002). Improved survival of *Lactobacillus paracasei* NFBC 338 in spray-dried powders containing gum acacia. *Journal of Applied Microbiology*, 93(6), 1003–1011. <https://doi.org/10.1046/j.1365-2672.2002.01782.x>
- FAO/WHO. (2002). *Joint FAO/WHO working group report on drafting guidelines for the evaluation of probiotics in food*. <http://ftp.fao.org/es/esn/food/wgreport2.pdf>.
- Fontes-Candia, C., Jiménez-Barrios, P., Miralles, B., Recio, I., López-Rubio, A., & Martínez-Sanz, M. (2022). Development of polysaccharide-casein gel-like structures resistant to in vitro gastric digestion. *Food Hydrocolloids*, 127, Article 107505. <https://doi.org/10.1016/j.foodhyd.2022.107505>
- Fortuin, J., Hellebois, T., Iken, M., Shaplov, A. S., Villas-Boas, S., Fogliano, V., et al. (2023). Study of the lyoprotective and stabilising effects of *Spirulina* (*Arthrospira platensis*) protein isolate on *Lactocaseibacillus rhamnosus* GG. In *Submitted to food hydrocolloids*.
- García-Brand, A. J., Quezada, V., Gonzalez-Melo, C., Bolaños-Barbosa, A. D., Cruz, J. C., & Reyes, L. H. (2022). Novel developments on stimuli-responsive probiotic encapsulates: From smart hydrogels to nanostructured platforms. *Fermentation*, 8(3), 117. <https://doi.org/10.3390/fermentation8030117>
- Gbassi, G. K., & Vandamme, T. (2012). Probiotic encapsulation technology: From microencapsulation to release into the gut. *Pharmaceutics*, 4(1). <https://doi.org/10.3390/pharmaceutics4010149>. Article 1.
- Georgantzopoulou, A., Serchi, T., Cambier, S., Leclercq, C. C., Renaut, J., Shao, J., et al. (2016). Effects of silver nanoparticles and ions on a co-culture model for the gastrointestinal epithelium. *Particle and Fibre Toxicology*, 13(1), 9. <https://doi.org/10.1186/s12989-016-0117-9>
- Giulio, B. D., Orlando, P., Barba, G., Coppola, R., Rosa, M. D., Sada, A., et al. (2005). Use of alginate and cryo-protective sugars to improve the viability of lactic acid bacteria after freezing and freeze-drying. *World Journal of Microbiology and Biotechnology*, 21(5), 739–746. <https://doi.org/10.1007/s11274-004-4735-2>
- Gomand, F., Borges, F., Burgain, J., Guerin, J., Revol-Junelles, A.-M., & Gaiani, C. (2019). Food matrix design for effective lactic acid bacteria delivery. *Annual Review of Food Science and Technology*, 10(1). <https://doi.org/10.1146/annurev-food-032818-121140>. Article 1.
- Gong, H., Gao, J., Wang, Y., Luo, Q. W., Guo, K. R., Ren, F. Z., et al. (2020). Identification of novel peptides from goat milk casein that ameliorate high-glucose-induced insulin resistance in HepG2 cells. *Journal of Dairy Science*, 103(6), 4907–4918. <https://doi.org/10.3168/jds.2019-17513>
- Gu, Q., Yin, Y., Yan, X., Liu, X., Liu, F., & McClements, D. J. (2022). Encapsulation of multiple probiotics, synbiotics, or nutraceuticals for improved health effects: A review. *Advances in Colloid and Interface Science*, 309, Article 102781. <https://doi.org/10.1016/j.cis.2022.102781>
- Guerrero Sanchez, M., Passot, S., Campoy, S., Olivares, M., & Fonseca, F. (2022). Effect of protective agents on the storage stability of freeze-dried *Ligilactobacillus salivarius* CECT5713. *Applied Microbiology and Biotechnology*, 106(21), 7235–7249. <https://doi.org/10.1007/s00253-022-12201-9>
- Haji, F., Cheon, J., Baek, J., Wang, Q., & Tam, K. C. (2022). Application of Pickering emulsions in probiotic encapsulation- A review. *Current Research in Food Science*, 5, 1603–1615. <https://doi.org/10.1016/j.crf.2022.09.013>
- Han, S., Lu, Y., Xie, J., Fei, Y., Zheng, G., Wang, Z., et al. (2021). Probiotic gastrointestinal transit and colonization after oral administration: A long journey. *Frontiers in Cellular and Infection Microbiology*, 11. <https://www.frontiersin.org/articles/10.3389/fcimb.2021.609722>.
- Hayes, M., Ross, R. P., Fitzgerald, G. F., Hill, C., & Stanton, C. (2006). Casein-derived antimicrobial peptides generated by *Lactobacillus acidophilus* DPC6026. *Applied and Environmental Microbiology*, 72(3), 2260–2264. <https://doi.org/10.1128/AEM.72.3.2260-2264.2006>
- Heidebach, T., Först, P., & Kulozik, U. (2009). Microencapsulation of probiotic cells by means of rennet-gelation of milk proteins. *Food Hydrocolloids*, 23(7), 1670–1677. <https://doi.org/10.1016/j.foodhyd.2009.01.006>
- Hellebois, T., Addiego, F., Gaiani, C., Shaplov, A. S., & Soukoulis, C. (2024). Unravelling the functionality of anionic and non-ionic plant seed gums on milk protein cryogels conveying *Lactocaseibacillus rhamnosus* GG. *Carbohydrate Polymers*, 323, Article 121376. <https://doi.org/10.1016/j.carbpol.2023.121376>
- Hellebois, T., Canuel, R., Addiego, F., Audinot, J.-N., Gaiani, C., Shaplov, A. S., et al. (2023). Milk protein-based cryogel monoliths as novel encapsulants of probiotic bacteria. Part I: Microstructural, physicochemical, and mechanical characterisation. *Food Hydrocolloids*, Article 108641. <https://doi.org/10.1016/j.foodhyd.2023.108641>
- Hellebois, T., Canuel, R., Leclercq, C. C., Gaiani, C., & Soukoulis, C. (2024). Milk protein-based cryogel monoliths as novel encapsulants of probiotic bacteria. Part II: *Lactocaseibacillus rhamnosus* GG storage stability and bioactivity under in vitro digestion. *Food Hydrocolloids*, 146, Article 109173. <https://doi.org/10.1016/j.foodhyd.2023.109173>
- Hellebois, T., Fortuin, J., Xu, X., Shaplov, A. S., Gaiani, C., & Soukoulis, C. (2021). Structure conformation, physicochemical and rheological properties of flaxseed gums extracted under alkaline and acidic conditions. *International Journal of Biological Macromolecules*, 192, 1217–1230. <https://doi.org/10.1016/j.ijbiomac.2021.10.087>
- Hellebois, T., Gaiani, C., Cambier, S., Noo, A., & Soukoulis, C. (2022). Exploration of the co-structuring and stabilising role of flaxseed gum in whey protein isolate based cryo-hydrogels. *Carbohydrate Polymers*, 289, Article 119424. <https://doi.org/10.1016/j.carbpol.2022.119424>
- Hellebois, T., Soukoulis, C., Xu, X., Hausman, J.-F., Shaplov, A., Taoukis, P. S., et al. (2021). Structure conformational and rheological characterisation of alfalfa seed (*Medicago sativa* L.) galactomannan. *Carbohydrate Polymers*, 256, Article 117394. <https://doi.org/10.1016/j.carbpol.2020.117394>
- Hill, C., Guarner, F., Reid, G., Gibson, G. R., Merenstein, D. J., Pot, B., et al. (2014). The International Scientific Association for Probiotics and Prebiotics consensus statement on the scope and appropriate use of the term probiotic. *Nature Reviews*

- Gastroenterology & Hepatology*, 11(8). <https://doi.org/10.1038/nrgastro.2014.66>. Article 8.
- Hiller, B., & Lorenzen, P. C. (2008). Surface hydrophobicity of physicochemically and enzymatically treated milk proteins in relation to techno-functional properties. *Journal of Agricultural and Food Chemistry*, 56(2), 461–468. <https://doi.org/10.1021/jf072400c>
- Iravani, S., Korbekandi, H., & Mirmohammadi, S. V. (2015). Technology and potential applications of probiotic encapsulation in fermented milk products. *Journal of Food Science and Technology*, 52(8), 4679–4696. <https://doi.org/10.1007/s13197-014-1516-2>
- Kieps, J., & Dembczyński, R. (2022). Current trends in the production of probiotic formulations. *Foods*, 11(15). <https://doi.org/10.3390/foods11152330>. Article 15.
- Kleemann, C., Schuster, R., Rosenecker, E., Selmer, I., Smirnova, I., & Kulozik, U. (2020). In-vitro-digestion and swelling kinetics of whey protein, egg white protein and sodium caseinate aerogels. *Food Hydrocolloids*, 101, Article 105534. <https://doi.org/10.1016/j.foodhyd.2019.105534>
- Kleemann, C., Selmer, I., Smirnova, I., & Kulozik, U. (2018). Tailor made protein based aerogel particles from egg white protein, whey protein isolate and sodium caseinate: Influence of the preceding hydrogel characteristics. *Food Hydrocolloids*, 83, 365–374. <https://doi.org/10.1016/j.foodhyd.2018.05.021>
- Kontogiorgos, V. (2019). Galactomannan (guar, locust bean, fenugreek, tara). In *Encyclopedia of food chemistry* (pp. 109–113). Elsevier. <https://doi.org/10.1016/B978-0-08-100596-5.21589-8>.
- Kuo, C.-C., Clark, S., Qin, H., & Shi, X. (2022). Development of a shelf-stable, gel-based delivery system for probiotics by encapsulation, 3D printing, and freeze-drying. *Lebensmittel-Wissenschaft & Technologie*, 157, Article 113075. <https://doi.org/10.1016/j.lwt.2022.113075>
- Lacroix, I. M. E., & Li-Chan, E. C. Y. (2014). Isolation and characterization of peptides with dipeptidyl peptidase-IV inhibitory activity from pepsin-treated bovine whey proteins. *Peptides*, 54, 39–48. <https://doi.org/10.1016/j.peptides.2014.01.002>
- Lacroix, I. M. E., Meng, G., Cheung, I. W. Y., & Li-Chan, E. C. Y. (2016). Do whey protein-derived peptides have dual dipeptidyl-peptidase IV and angiotensin I-converting enzyme inhibitory activities? *Journal of Functional Foods*, 21, 87–96. <https://doi.org/10.1016/j.jff.2015.11.038>
- Lira, M. M., Oliveira Filho, J. G. de, Sousa, T. L. de, Costa, N. M. da, Lemes, A. C., Fernandes, S. S., et al. (2023). Selected plants producing mucilage: Overview, composition, and their potential as functional ingredients in the development of plant-based foods. *Food Research International*, 169, Article 112822. <https://doi.org/10.1016/j.foodres.2023.112822>
- Liu, J., Shim, Y. Y., Tse, T. J., Wang, Y., & Reaney, M. J. T. (2018). Flaxseed gum a versatile natural hydrocolloid for food and non-food applications. *Trends in Food Science & Technology*, 75, 146–157. <https://doi.org/10.1016/j.tifs.2018.01.011>
- Liu, Y., Liu, B., Li, D., Hu, Y., Zhao, L., Zhang, M., ... Li, Y. (2020). Improved Gastric Acid Resistance and Adhesive Colonization of Probiotics by Mucoadhesive and Intestinal Targeted Konjac Glucomannan Microspheres. *Adv. Funct. Mater.*, 30, 2001157. [doi:10.1002/adfm.202001157](https://doi.org/10.1002/adfm.202001157).
- Lozinsky, V. I. (2018). Cryostructuring of polymeric systems. 50. † cryogels and cryotropic gel-formation: Terms and definitions. *Gels*, 4(3), 77. <https://doi.org/10.3390/gels4030077>
- Luo, J., Li, Y., Mai, Y., Gao, L., Ou, S., Wang, Y., et al. (2018). Flaxseed gum reduces body weight by regulating gut microbiota. *Journal of Functional Foods*, 47, 136–142. <https://doi.org/10.1016/j.jff.2018.05.042>
- Manzocco, L., Mikkonen, K. S., & García-González, C. A. (2021). Aerogels as porous structures for food applications: Smart ingredients and novel packaging materials. *Food Structure*, 28, Article 100188. <https://doi.org/10.1016/j.foostr.2021.100188>
- Markussen, J. Ø., Madsen, F., Young, J. F., & Corredig, M. (2021). A semi dynamic in vitro digestion study of milk protein concentrate dispersions structured with different polysaccharides. *Current Research in Food Science*, 4, 250–261. <https://doi.org/10.1016/j.crf.2021.03.012>
- Mays, Z. J. S., Chappell, T. C., & Nair, N. U. (2020). Quantifying and engineering mucus adhesion of probiotics. *ACS Synthetic Biology*, 9(2), 356–367. <https://doi.org/10.1021/acssynbio.9b00356>
- Mendonça, A. A., Pinto-Neto, W. de P., da Paixão, G. A., Santos, D. da S., De Moraes, M. A., & De Souza, R. B. (2023). Journey of the probiotic bacteria: Survival of the fittest. *Microorganisms*, 11(1). <https://doi.org/10.3390/microorganisms11010095>. Article 1.
- Minkiewicz, P., Iwaniak, A., & Darewicz, M. (2019). BIOPEP-UWM database of bioactive peptides: Current opportunities. *International Journal of Molecular Sciences*, 20(23). <https://doi.org/10.3390/ijms20235978>. Article 23.
- Mueed, A., Shibli, S., Korma, S. A., Madjirebaye, P., Esatbeyoglu, T., & Deng, Z. (2022). Flaxseed bioactive compounds: Chemical composition, functional properties, food applications and health benefits-related gut microbes. *Foods*, 11(20). <https://doi.org/10.3390/foods11203307>. Article 20.
- Oluwatofin, S. O., Tai, S. L., & Fagan-Endres, M. A. (2022). Sucrose, maltodextrin and inulin efficacy as cryoprotectant, preservative and prebiotic – towards a freeze dried *Lactobacillus plantarum* topical probiotic. *Biotechnology Reports*, 33, Article e00696. <https://doi.org/10.1016/j.btre.2021.e00696>
- O'Sullivan, J., Arellano, M., Pichot, R., & Norton, I. (2014). The effect of ultrasound treatment on the structural, physical and emulsifying properties of dairy proteins. *Food Hydrocolloids*, 42, 386–396. <https://doi.org/10.1016/j.foodhyd.2014.05.011>
- Peredo, A. G., Beristain, C. I., Pascual, L. A., Azuara, E., & Jimenez, M. (2016). The effect of prebiotics on the viability of encapsulated probiotic bacteria. *Lebensmittel-Wissenschaft & Technologie*, 73, 191–196. <https://doi.org/10.1016/j.lwt.2016.06.021>
- Power, O., Fernández, A., Norris, R., Riera, F. A., & FitzGerald, R. J. (2014). Selective enrichment of bioactive properties during ultrafiltration of a tryptic digest of β-lactoglobulin. *Journal of Functional Foods*, 9, 38–47. <https://doi.org/10.1016/j.jff.2014.04.002>
- Prajapati, V. D., Jani, G. K., Moradiya, N. G., Randeria, N. P., Nagar, B. J., Naikvadi, N. N., et al. (2013). Galactomannan: A versatile biodegradable seed polysaccharide. *International Journal of Biological Macromolecules*, 60, 83–92. <https://doi.org/10.1016/j.ijbiomac.2013.05.017>
- Qian, K. Y., Cui, S. W., Wu, Y., & Goff, H. D. (2012). Flaxseed gum from flaxseed hulls: Extraction, fractionation, and characterization. *Food Hydrocolloids*, 28(2), 275–283. <https://doi.org/10.1016/j.foodhyd.2011.12.019>
- Quiros, A., Ramos, M., Muguerza, B., Delgado, M. A., Miguel, M., Aleixandre, A., et al. (2007). Identification of novel antihypertensive peptides in milk fermented with *Enterococcus faecalis*. *International Dairy Journal*, 17(1), 33–41. <https://doi.org/10.1016/j.idairyj.2005.12.011>
- Raddatz, G. C., Poletto, G., Deus, C. de, Codevilla, C. F., Cichoski, A. J., Jacob-Lopes, E., et al. (2020). Use of prebiotic sources to increase probiotic viability in pectin microparticles obtained by emulsification/internal gelation followed by freeze-drying. *Food Research International*, 130, Article 108902. <https://doi.org/10.1016/j.foodres.2019.108902>
- Reddi, S., Shanmugam, V. P., Tanedjeu, K. S., Kapila, S., & Kapila, R. (2018). Effect of buffalo casein-derived novel bioactive peptides on osteoblast differentiation. *European Journal of Nutrition*, 57(2), 593–605. <https://doi.org/10.1007/s00394-016-1346-2>
- Ries, D., Ye, A., Haisman, D., & Singh, H. (2010). Antioxidant properties of caseins and whey proteins in model oil-in-water emulsions. *International Dairy Journal*, 20(2), 72–78. <https://doi.org/10.1016/j.idairyj.2009.09.001>
- Robert, M.-C., Razaname, A., Mutter, M., & Juillerat, M. A. (2004). Identification of angiotensin-I-converting enzyme inhibitory peptides derived from sodium caseinate hydrolysates produced by *Lactobacillus helveticus* NCC 2765. *Journal of Agricultural and Food Chemistry*, 52(23), 6923–6931. <https://doi.org/10.1021/jf049510t>
- Sanders, M. E., & Marco, M. L. (2010). Food formats for effective delivery of probiotics. *Annual Review of Food Science and Technology*, 1(1), 65–85. <https://doi.org/10.1146/annurev.food.080708.100743>
- sekhavatizadeh, S. S., Pourakbar, N., Ganje, M., Shekarfroush, S. S., & Hosseinzadeh, S. (2023). Physicochemical and sensory properties of probiotic yogurt containing *Lactobacillus plantarum* ATCC 10241 microencapsulated with okra (*Abelmoschus esculentus*) mucilage and sodium alginate. *Bioactive Carbohydrates and Dietary Fibre*, 30, Article 100364. <https://doi.org/10.1016/j.bcdf.2023.100364>
- Silveira, S. T., Martínez-Maqueda, D., Recio, I., & Hernández-Ledesma, B. (2013). Dipeptidyl peptidase-IV inhibitory peptides generated by tryptic hydrolysis of a whey protein concentrate rich in β-lactoglobulin. *Food Chemistry*, 141(2), 1072–1077. <https://doi.org/10.1016/j.foodchem.2013.03.056>
- Soukoulis, C., Gaiani, C., & Hoffmann, L. (2018). Plant seed mucilage as emerging biopolymer in food industry applications. *Current Opinion in Food Science*, 22, 28–42. <https://doi.org/10.1016/j.cofs.2018.01.004>
- Sun, H., Zhang, M., Liu, Y., Wang, Y., Chen, Y., Guan, W., et al. (2021). Improved viability of *Lactobacillus plantarum* embedded in whey protein concentrate/pullulan/trehalose hydrogel during freeze drying. *Carbohydrate Polymers*, 260, Article 117843. <https://doi.org/10.1016/j.carbpol.2021.117843>
- Świątecka, D., Małgorzata, I., Aleksander, Ś., Henryk, K., & Elżbieta, K. (2010). The impact of glycated pea proteins on bacterial adhesion. *Food Research International*, 43(6), 1566–1576. <https://doi.org/10.1016/j.foodres.2010.03.003>
- Tauzin, J., Miclo, L., & Gaillard, J.-L. (2002). Angiotensin-I-converting enzyme inhibitory peptides from tryptic hydrolysate of bovine α2-casein. *FEBS Letters*, 531(2), 369–374. [https://doi.org/10.1016/S0014-5793\(02\)03576-7](https://doi.org/10.1016/S0014-5793(02)03576-7)
- Torres-Fuentes, C., Schellekens, H., Dinan, T. G., & Cryan, J. F. (2017). The microbiota–gut–brain axis in obesity. *The Lancet Gastroenterology & Hepatology*, 2(10), 747–756. [https://doi.org/10.1016/S2468-1253\(17\)30147-4](https://doi.org/10.1016/S2468-1253(17)30147-4)
- Tripathi, P., Beaussart, A., Alsteens, D., Dupres, V., Claes, I., von Ossowski, I., et al. (2013). Adhesion and nanomechanics of pili from the probiotic *Lactobacillus rhamnosus* GG. *ACS Nano*, 7(4), 3685–3697. <https://doi.org/10.1021/nn400705u>
- Tu, M., Liu, H., Zhang, R., Chen, H., Mao, F., Cheng, S., et al. (2018). Analysis and evaluation of the inhibitory mechanism of a novel angiotensin-I-converting enzyme inhibitory peptide derived from casein hydrolysate. *Journal of Agricultural and Food Chemistry*, 66(16), 4139–4144. <https://doi.org/10.1021/acs.jafc.8b00732>
- Udechukwu, M. C., Dang, C., & Udenigwe, C. C. (2021). Identification of zinc-binding peptides in ADAM17-inhibiting whey protein hydrolysates using IMAC-Zn²⁺ coupled with shotgun peptidomics. *Food Production, Processing and Nutrition*, 3(1), 5. <https://doi.org/10.1186/s43014-020-00048-4>
- van Boekel, M. (2002). On the use of the Weibull model to describe thermal inactivation of microbial vegetative cells. *International Journal of Food Microbiology*, 74(1–2), 139–159. [https://doi.org/10.1016/S0168-1605\(01\)00742-5](https://doi.org/10.1016/S0168-1605(01)00742-5)
- Vargas, L. A., Olson, D. W., & Aryana, K. J. (2015). Whey protein isolate improves acid and bile tolerances of *Streptococcus thermophilus* ST-M5 and *Lactobacillus delbrueckii* ssp. *Bulgarius* LB-12. *Journal of Dairy Science*, 98(4), 2215–2221. <https://doi.org/10.3168/jds.2014-8869>
- Venema, K., & Carmo, A. P. do (2015). Probiotics and prebiotics: Current status and future trends. In *Probiotics and Prebiotics: Current research and future trends* (pp. 3–12). Caister Academic Press. <https://doi.org/10.21775/9781910190098.01>
- Ventura, M., Margolles, A., Turrioni, F., Zomer, A., de los Reyes-Gavilán, C. G., & van Sinderen, D. (2011). Stress responses of bifidobacteria. In E. Tsakalidou, & K. Papanimitrou (Eds.), *Stress responses of lactic acid bacteria* (pp. 323–347). Springer US. https://doi.org/10.1007/978-0-387-92771-8_14
- Volkova, N., & Berillo, D. (2021). Water uptake as a crucial factor on the properties of cryogels of gelatine cross-linked by dextran dialdehyde. *Gels*, 7(4), 159. <https://doi.org/10.3390/gels7040159>

- Wendel, U. (2022). Assessing viability and stress tolerance of probiotics—a review. *Frontiers in Microbiology*, 12. <https://www.frontiersin.org/articles/10.3389/fmicb.2021.818468>.
- Wu, Y., Cui, W., Eskin, N. A. M., & Goff, H. D. (2009). Fractionation and partial characterization of non-pectic polysaccharides from yellow mustard mucilage. *Food Hydrocolloids*, 23(6), 1535–1541. <https://doi.org/10.1016/j.foodhyd.2008.10.010>
- Yao, H., Liu, B., He, L., Hu, J., & Liu, H. (2023). The incorporation of peach gum polysaccharide into soy protein based microparticles improves probiotic bacterial survival during simulated gastrointestinal digestion and storage. *Food Chemistry*, 413, Article 135596. <https://doi.org/10.1016/j.foodchem.2023.135596>
- Yin, M., Chen, M., Yuan, Y., Liu, F., & Zhong, F. (2024). Encapsulation of *Lactobacillus rhamnosus* GG in whey protein isolate-shortening oil and gum Arabic by complex coacervation: Enhanced the viability of probiotics during spray drying and storage. *Food Hydrocolloids*, 146, Article 109252. <https://doi.org/10.1016/j.foodhyd.2023.109252>
- Yin, X., Cheng, H., Wusigale, Dong, H., Huang, W., & Liang, L. (2022). Resveratrol stabilization and loss by sodium caseinate, whey and soy protein isolates: Loading, antioxidant activity, oxidability. *Antioxidants*, 11(4), 647. <https://doi.org/10.3390/antiox11040647>
- Zhu, Q., Tang, J., Yao, S., Feng, J., Mi, B., Zhu, W., et al. (2023). Controllable structure of porous starch facilitates bioactive encapsulation by mild gelatinization. *Food Hydrocolloids*, 145, Article 109135. <https://doi.org/10.1016/j.foodhyd.2023.109135>